On the road to extreme radiation hardness with the innovative batch of FBK nLGADs

Gain and timing performances from beam tests

Robert White **04/09/26**

Torino (University, INFN, UNIPO): Anna Rita Altamura, Roberta Arcidiacono, Nicolò Cartiglia, Matteo Durando, Marco Ferrero, Simone Galletto, Leonardo Lanteri, Ludovico Massaccesi, Margherita Obertino, Nadia Pastrone, Federico Siviero, Valentina Sola, Marta Tornago

Perugia (University, INFN, CNR-ION): Tommaso Croci, Alessandro Fondacci, Ariana Morozzi, Francesco Moscatelli, Daniele Passeri

Trento (FBK, Trento Institute): Omar Hammad Ali, Ashish Bisht, Maurizio Boscardin, Matteo Centis Vignali, Giovanni Paternoster, Syed Muhammad Abouzar Sarfraz

PSD14 Conference
1st - 4th September 2026

Funded by the European Union

The motivation for innovation in silicon detectors

- Future collider experiments (**HL-LHC, FCC-hh**) will reach higher **luminosities** and **energies**
- Current silicon pixel and strip detectors cannot withstand such **high fluence environments**
  - HL-LHC ATLAS detector will experience 3.5 x 10^{16} $n_{eq}cm^{-2}$
  - FCC-hh expected to hit ~10^{18} $n_{eq}cm^{-2}$

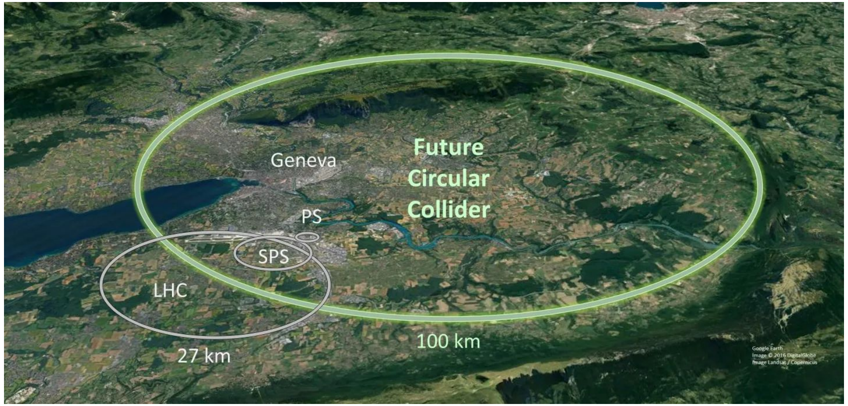

Seek a highly **radiation-hard** detector design

- **Thin substrate** for prompt signal and less damage
- **Precise doping engineering** to reduce radiation effects

One such device that meets these criteria is the **low-gain avalanche diode (LGAD)**

Refs.: [1] *HL-LHC*, [2] *CMS*, [3] *ATLAS*, [4] *FCC-hh*

- **The n-type LGAD**
- The FBK NLGAD batch of sensors
- Temperature characterisation of the FBK NLGAD batch
- Operations at the DESY and CERN SPS Test Beam Facilities
- Timing performances of the FBK NLGAD batch

Standard p-type LGAD widely established

- e^- **drift** within bulk to gain layer
- e^- trigger avalanche

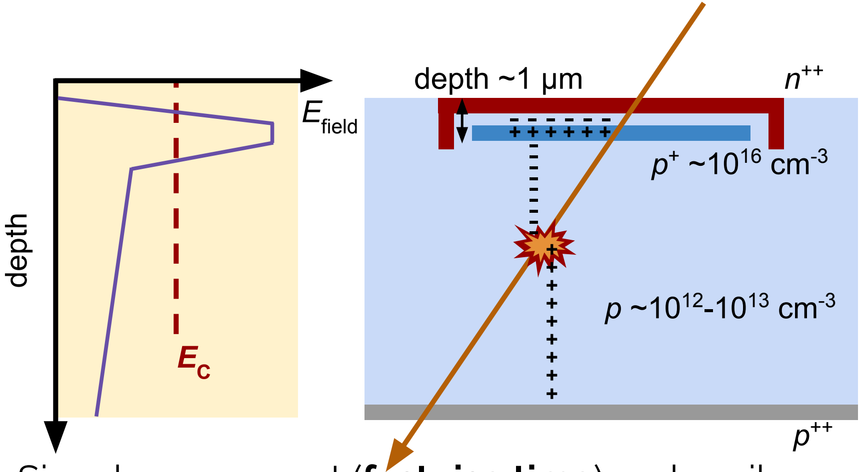

Signals are prompt (**fast rise time**) and easily characterised (**no prolonged peaks**)

- e^- drift on rising edge, h^+ return on falling edge

Standard p-type LGAD widely established

- e^- **drift** within bulk to gain layer
- e^- trigger avalanche

n-type LGAD (NLGAD) less established

- h^+ **drift** within bulk to gain layer
- h^+ trigger avalanche

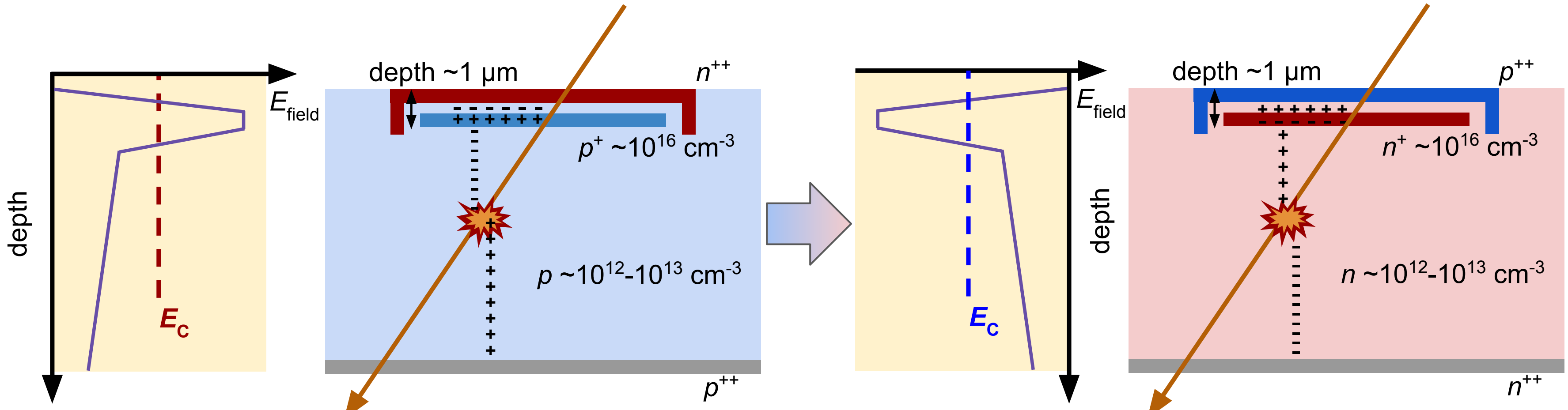

Signals are prompt (**fast rise time**) and easily characterised (**no prolonged peaks**)

- e^- drift on rising edge, h^+ return on falling edge

Signals are generally slower (**long rise time**) and broader (**higher shot noise, h^+ mobility lower**)

- h^+ drift on rising edge, e^- return on falling edge

Standard p-type LGAD widely established

- e^- **drift** within bulk to gain layer
- e^- trigger avalanche

n-type LGAD (NLGAD) less established

- h^+ **drift** within bulk to gain layer
- h^+ **trigger avalanche**

This is *greatly oversimplifying* the reality of going from p-type to n-type

- e^- have a **lower impact ionisation** coefficient than h^+
- The **effect on the multiplication** will therefore change
- e^- and h^+ **mobilities are different**
- Full v_{drift} saturation for h^+ requires >5-10 Vμm^{-1}, but is **sufficiently stable at >2 Vμm^{-1}**

NLGADs are **intrinsically noisier** devices than LGADs

- **Shot noise higher**
- **E-field** required for multiplication **higher**

Refs.: [5] Pellegrini et. al., LGADs for HEP applications
[6] M. Moll, TCAD simulation of impact ionisation
[7] E. Rivera, M. Moll, Impact ionisation coefficients in LGADs
[8] C. Canali et. al., Hole drift velocity in silicon

Higher gain from **e⁻** charge carriers

- Those that reach *n*$^+$ borne in *p*$^{++}$ contact
  - Contact not depleted
  - **Diffusion** rather than drift

Soft X-rays < 1 keV absorbed within ~1-2 μm

- For **low-penetrating particles**, NLGADs are superior to *p*-type LGADs for **position** and **timing resolution**
  - *p*-type avalanche is initiated by h$^+$ in this region

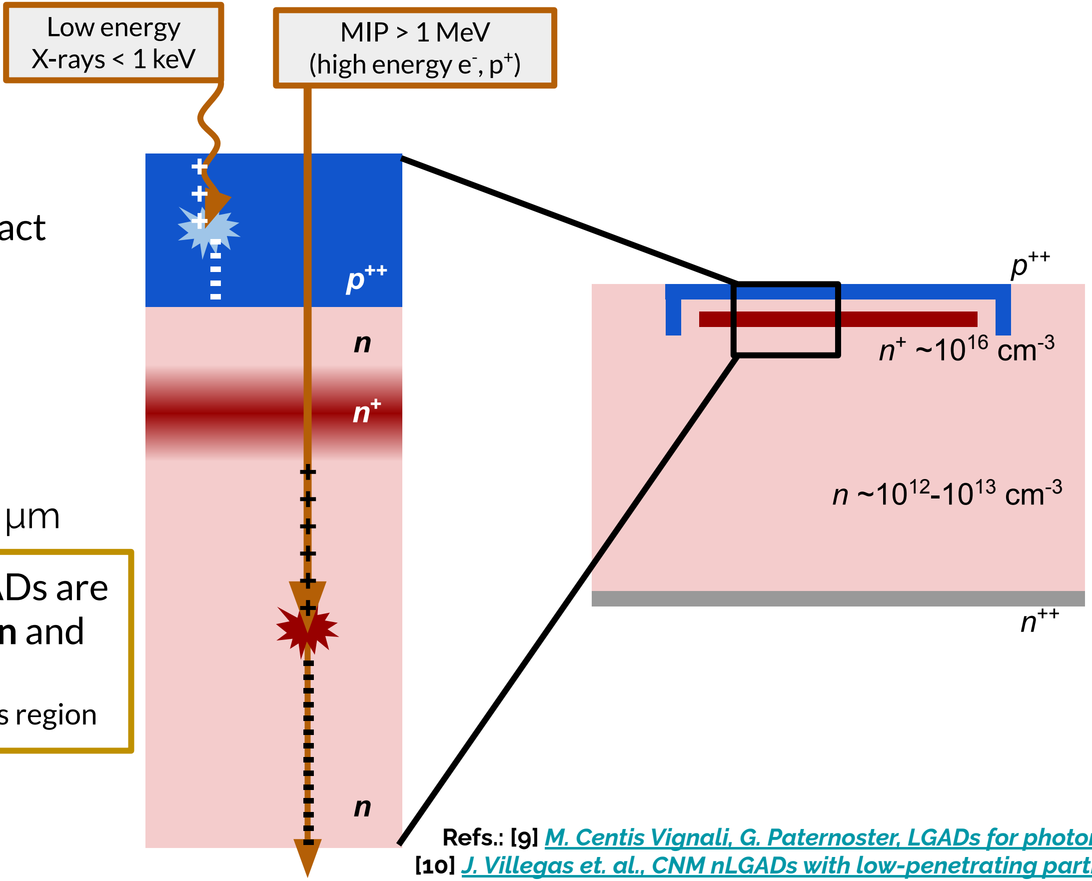

Refs.: [9] M. Centis Vignali, G. Paternoster, LGADs for photons
[10] J. Villegas et. al., CNM nLGADs with low-penetrating particles

NLGADs will also help in the development of **compensated LGADs**

- Peak doping concentration of the gain layer degrades under irradiation

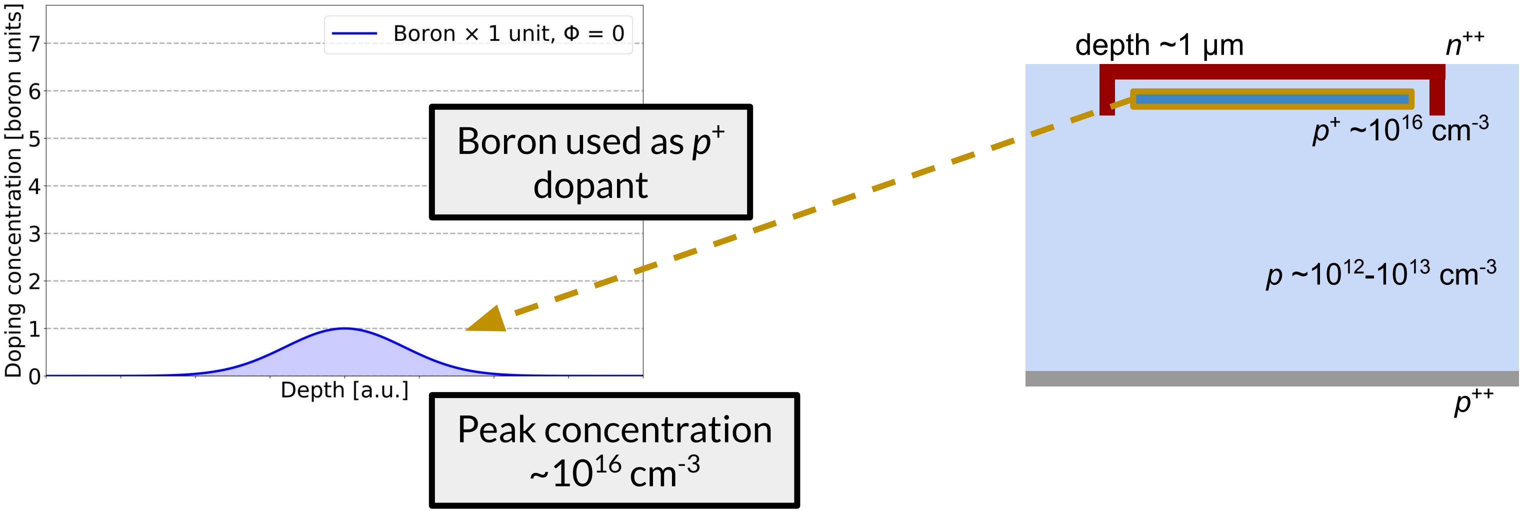

NLGADs will also help in the development of **compensated LGADs**

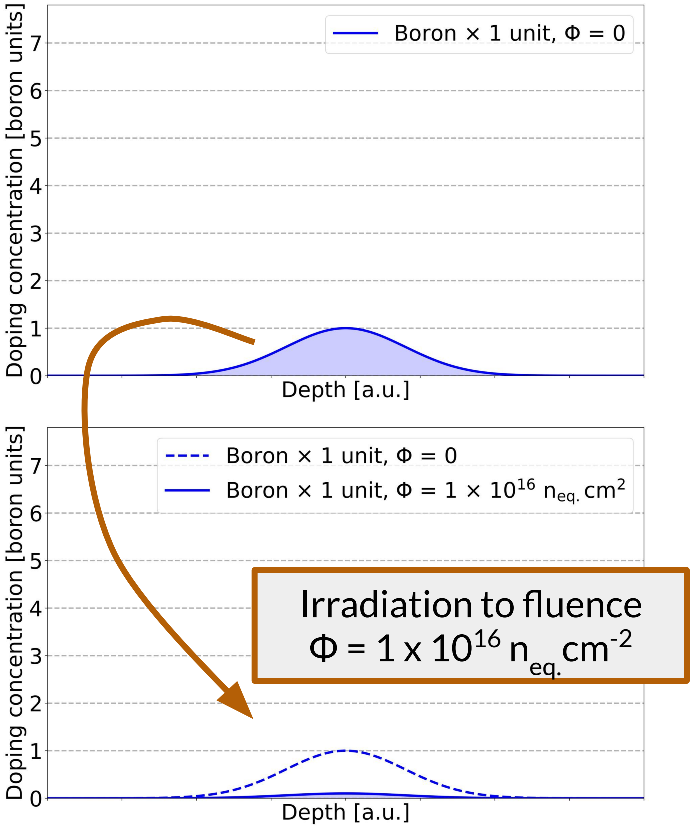

- Peak doping concentration of the gain layer degrades under irradiation
- **Acceptor (*p*⁺) removal rate** means boron quickly becomes **electronically deactivated**
- Acceptor removal mechanism well-characterised in **FBK pLGADs**

Can *compensate* for this with a sub-population of **donors (*n*⁺)**

NLGADs will also help in the development of **compensated LGADs**

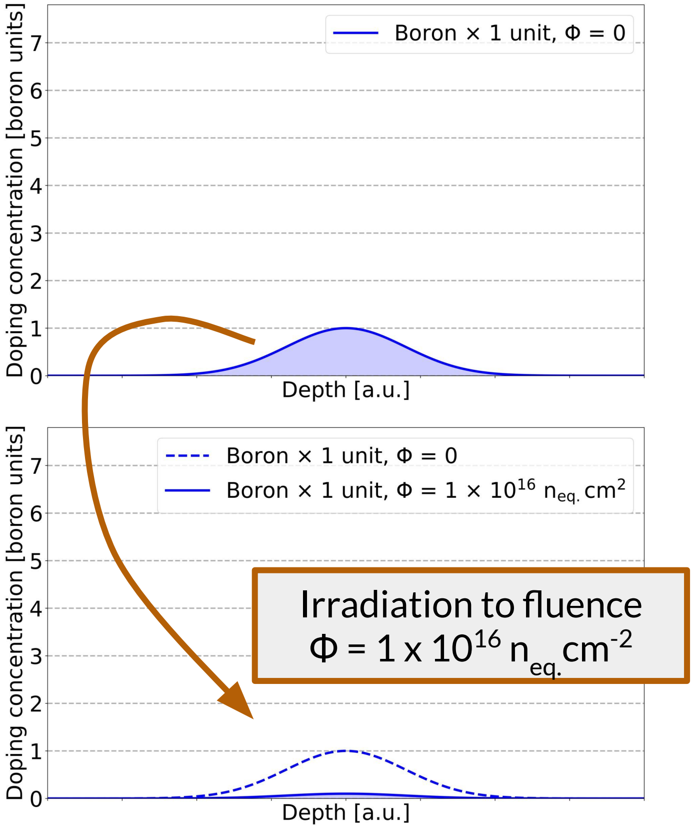

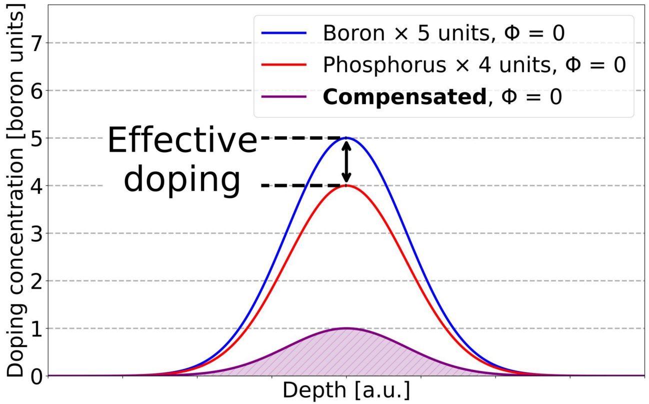

Can *compensate* for this with a sub-population of **donors (n^+)**

- Highly doped boron concentration (5 times nominal)
- Co-doped with **phosphorus** concentration (**ratio 5:4**)
- Now have an **effective difference in doping**

NLGADs will also help in the development of **compensated LGADs**

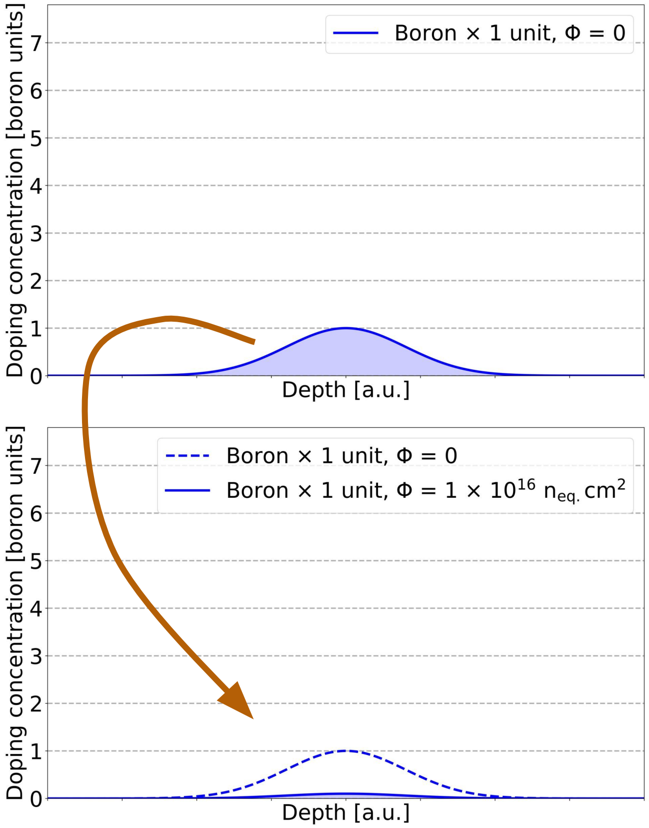

Interplay between acceptor and donor removal mechanisms unknown

- **Donor removal mechanism** can be probed in NLGADs
- Novelty for doping densities **~10^{15}-10^{17} cm^{-3}**
- How **rate** compares to acceptor removal

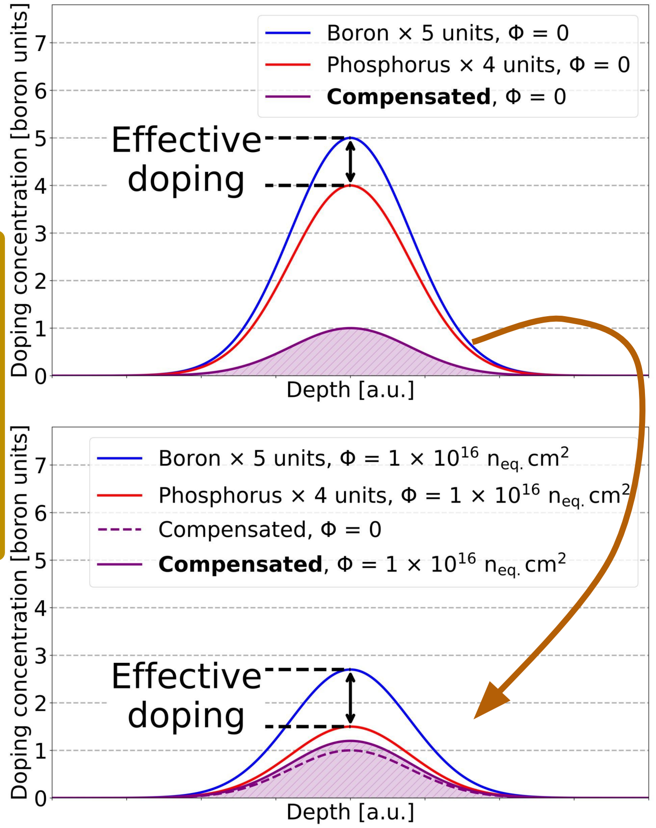

- The n-type LGAD
- **The FBK NLGAD batch of sensors**
- Temperature characterisation of the FBK NLGAD batch
- Operations at the DESY and CERN SPS Test Beam Facilities
- Timing performances of the FBK NLGAD batch

FBK NLGAD batch of sensors left foundry Nov 2025

- **55 µm-thick, >10 kΩcm** epitaxial on *n*-doped (phosphorus) substrate

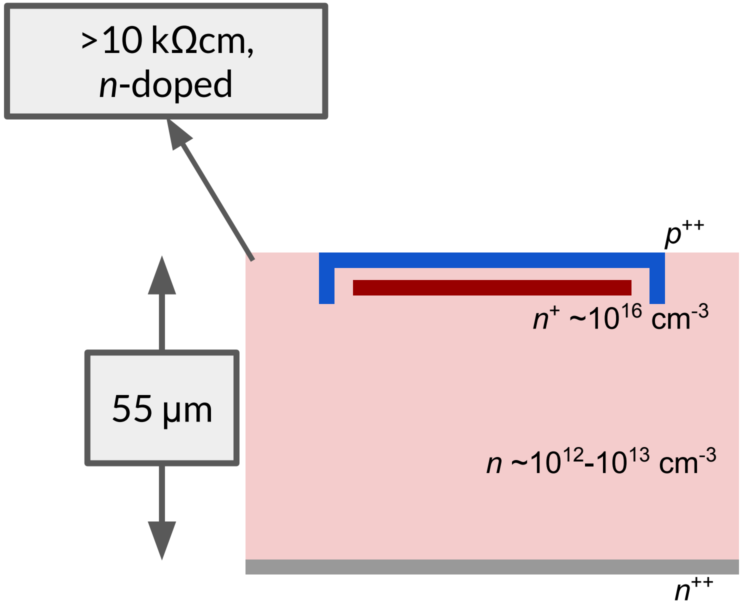

FBK NLGAD batch of sensors left foundry Nov 2025

- **55 µm-thick, >10 kΩcm** epitaxial on *n*-doped (phosphorus) substrate

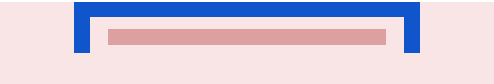

Novel ***p***$^{++}$ **ohmic contact** design

- Various *p*$^{++}$ diffusion modes simulated
- Short-loop runs and SIMS to tune profiles

p^{++} profiles – Process simulation

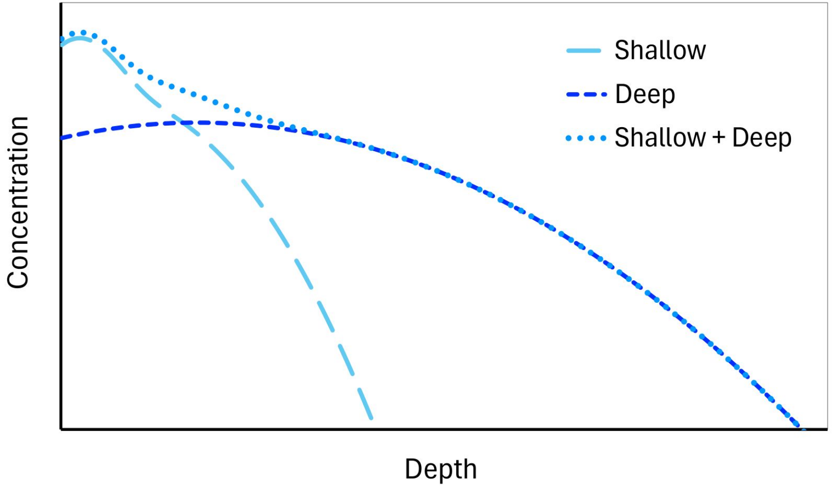

p^{++}**: shallow**, **deep**, and combined (**shallow+deep**) designs feature in the batch

FBK NLGAD batch of sensors left foundry Nov 2025

- **55 µm-thick, >10 kΩcm** epitaxial on *n*-doped (phosphorus) substrate

Novel ***p***$^{++}$ **ohmic contact** design

- Various *p*$^{++}$ diffusion modes simulated
- Short-loop runs and SIMS to tune profiles

Different ***n***$^{+}$ **implant** designs

- Simulated over a wide range of implantation energies
- Profiles tuned with EXFLU1 SIMS

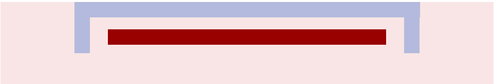

n^{+} profiles – Process simulation

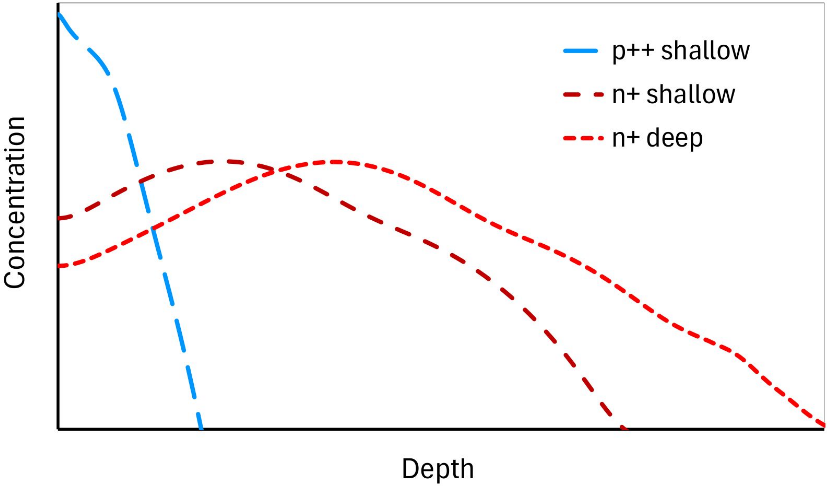

n^{++}**:** gain implant species **phosphorus** (shallow, deep) and **arsenic** (shallow only) (graphic for equal *n*$^{+}$ dose here)

FBK NLGAD batch of sensors left foundry Nov 2025

- **55 µm-thick, >10 kΩcm** epitaxial on *n*-type (phosphorus) substrate
- Considerations for the resulting **periphery design**

No floating GRs 1 floating GR 3 floating GRs

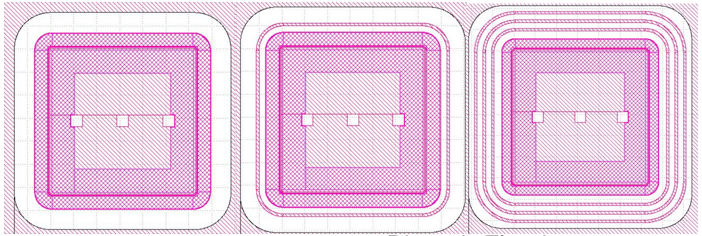

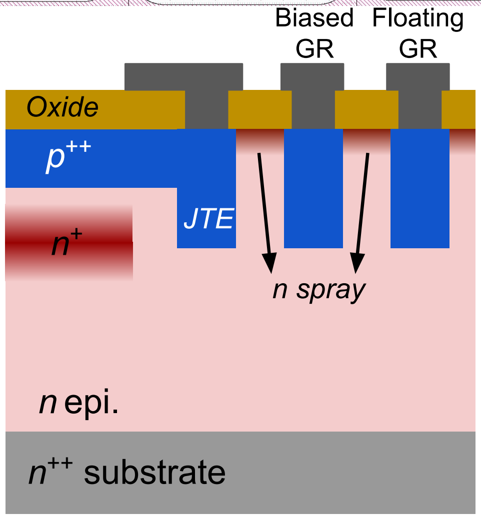

Ten combinations of periphery design have been tested via TCAD simulation and IV studies

- Group into none, 1, or 3 **floating guard rings (GRs)**
  - GRs to taper internal *E*-field
- ***n*-stop**, ***n*-spray (high or low dose)**, or no *n*-type isolation
  - Prevent effects of surface damage

Refs. on the electrical characterisation of FBK NLGADs:
[11] *V. Sola et. al., The path to the extreme fluences via the nLGAD sensors*
[12] *A. R. Altamura et. al., Results from the first 55 µm thick nLGAD sensors from FBK*
[13] *L. Massaccesi et. al., Characterisation of the first 55 µm thick nLGAD sensors from FBK*

Ref. on periphery studies with the FBK *p*-type LGADs:
[14] *A. R. Altamura et. al., Periphery layout strategies to mitigate discharges in thin silicon sensors*

Wafer	Contact	Gain	n^+ dose	*Families*
1	Shallow	Phosphorus shallow	1.20	Shallow contact + shallow P gain
2			1.26	
3			1.30	
4			1.36	
5			1.40	
6	Deep or Shallow+Deep	Phosphorus deep	1.30	Deep/S+D contact + deep P gain
7			1.36	
9			1.40	
10	Shallow		0.90	Shallow contact + deep P gain
11			0.96	
12			1.00	
13		Arsenic shallow	1.30	Shallow contact + shallow As gain
14			1.36	
15			1.40	

No beam test results as $V_{bd} < 100$ V

<table>
<tr><th>Wafer</th><th>Contact</th><th>Gain</th><th>n^+ dose</th></tr>
<tr><td>1</td><td rowspan="5">Shallow</td><td rowspan="5">Phosphorus shallow</td><td>1.20</td></tr>
<tr><td>2</td><td>1.26</td></tr>
<tr><td>3</td><td>1.30</td></tr>
<tr><td>4</td><td>1.36</td></tr>
<tr><td>5</td><td>1.40</td></tr>
<tr><td>6</td><td rowspan="3">Deep or Shallow+Deep</td><td rowspan="6">Phosphorus deep</td><td>1.30</td></tr>
<tr><td>7</td><td>1.36</td></tr>
<tr><td>9</td><td>1.40</td></tr>
<tr><td>10</td><td rowspan="6">Shallow</td><td>0.90</td></tr>
<tr><td>11</td><td>0.96</td></tr>
<tr><td>12</td><td>1.00</td></tr>
<tr><td>13</td><td rowspan="3">Arsenic shallow</td><td>1.30</td></tr>
<tr><td>14</td><td>1.36</td></tr>
<tr><td>15</td><td>1.40</td></tr>
</table>

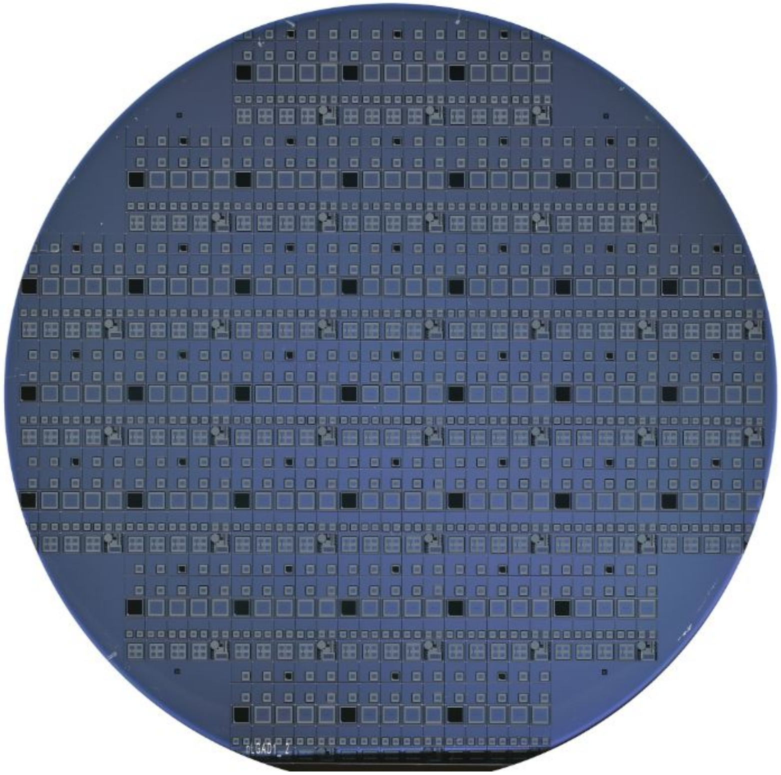

FBK NLGAD wafer

Wafer	Contact	Gain	n^+ dose
1	Shallow	Phosphorus shallow	1.20
2			1.26
3			1.30
4			1.36
5			1.40
6	Deep or Shallow+Deep	Phosphorus deep	1.30
7			1.36
9			1.40
10	Shallow		0.90
11			0.96
12			1.00
13		Arsenic shallow	1.30
14			1.36
15			1.40

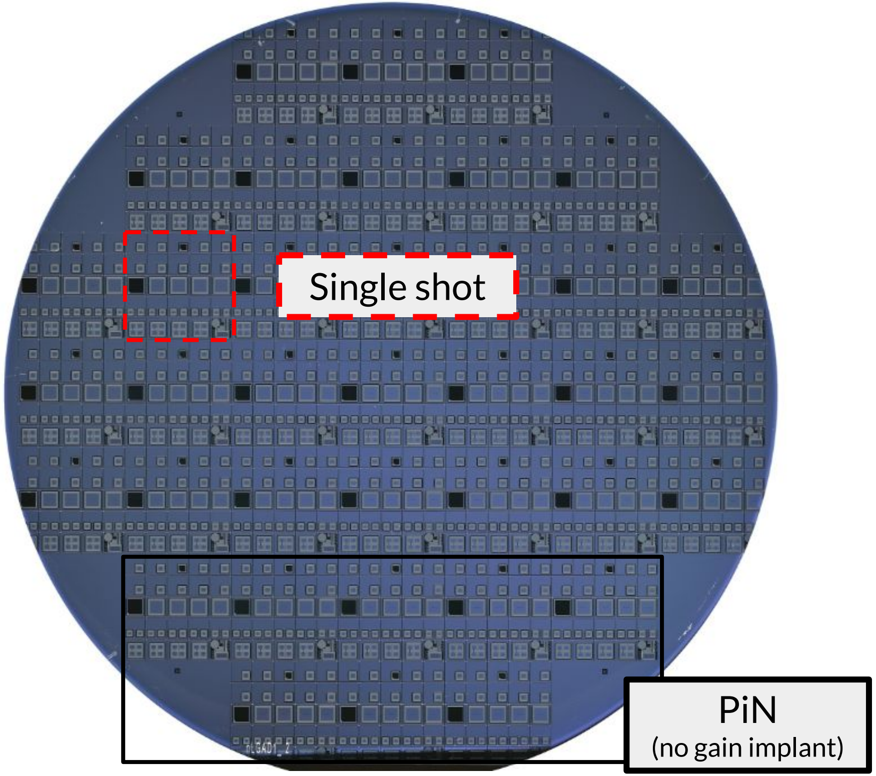

FBK NLGAD wafer

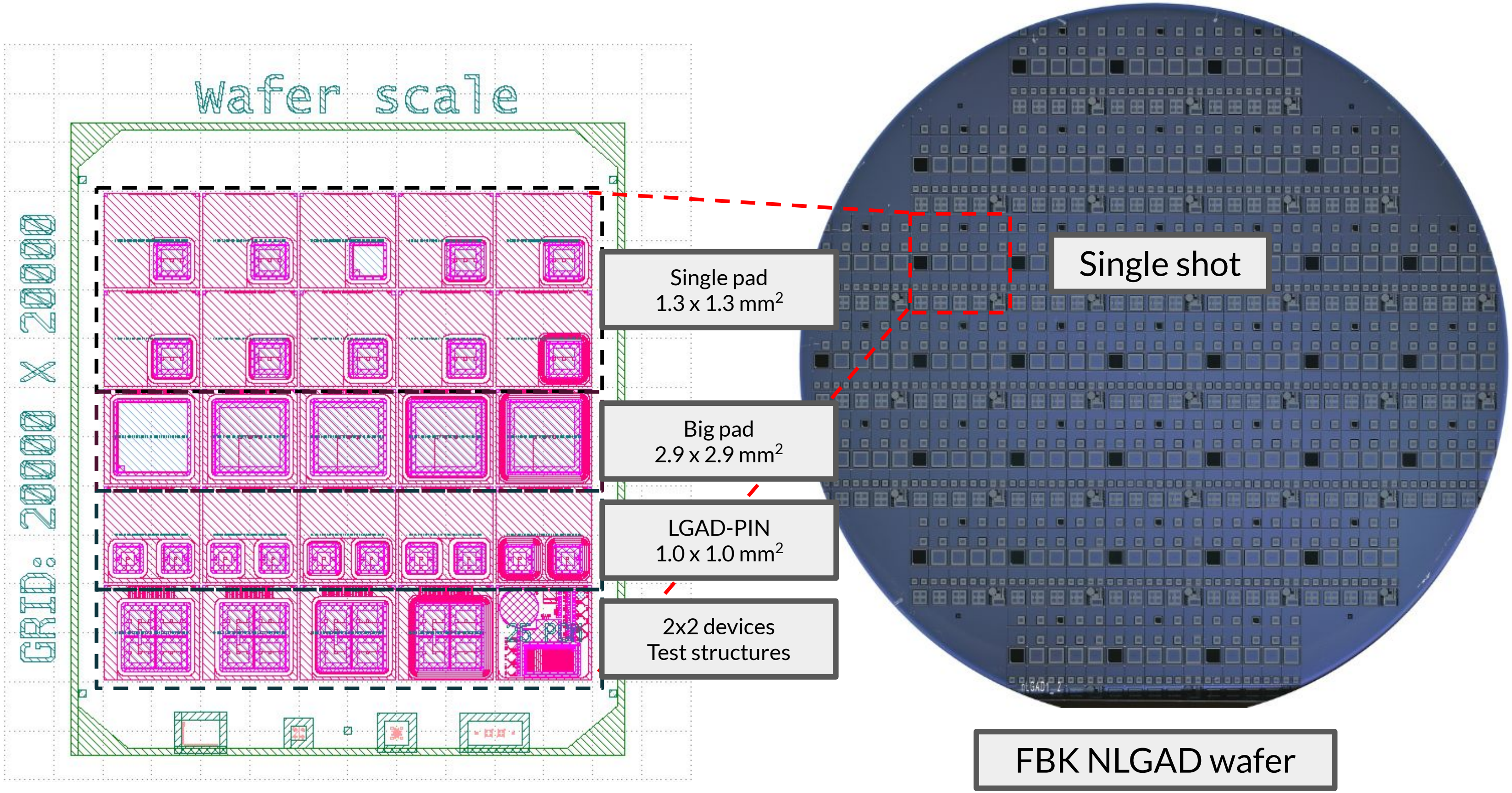
Wafer scale
GRID: 20000 X 20000
Single pad
1.3 x 1.3 mm^2
Big pad
2.9 x 2.9 mm^2
LGAD-PIN
1.0 x 1.0 mm^2
2x2 devices
Test structures
Single shot
FBK NLGAD wafer

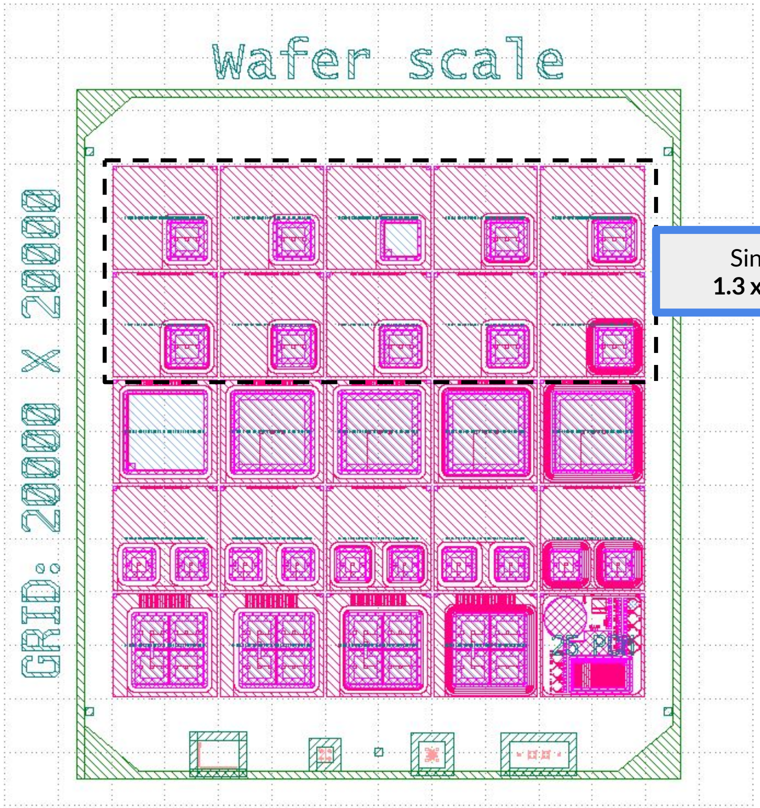

Single pad
1.3 x 1.3 mm^2

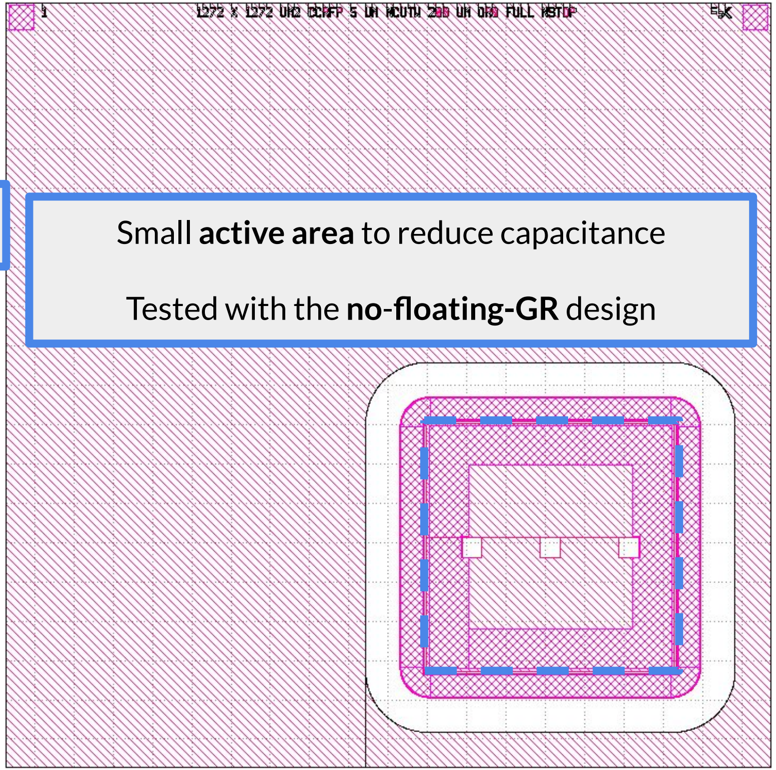

Small **active area** to reduce capacitance

Tested with the **no-floating-GR** design

- The n-type LGAD
- The FBK NLGAD batch of sensors
- **Temperature characterisation of the FBK NLGAD batch**
- Operations at the DESY and CERN SPS Test Beam Facilities
- Timing performances of the FBK NLGAD batch

Performed **^{90}Sr** (MIP, β source) measurements at 10˚C intervals between -30 and 30˚C

- Calculate **charge collected** at each bias point per set temperature
- Data acquisition identical to beam test
  - 1 GHz BW, 20 dB Cividec amplifier
  - SC readout board (integ. 20 dB amplification)
  - LeCroy 4-channel oscilloscope

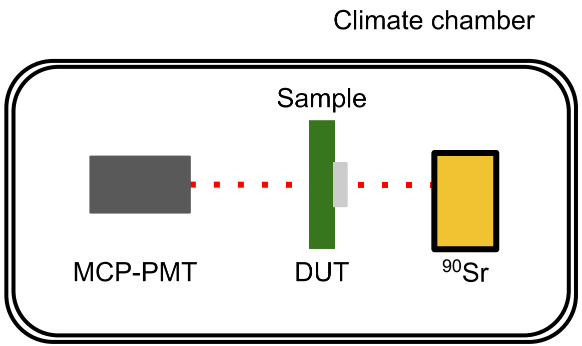

Performed ^{90}**Sr** (MIP, β source) measurements at 10˚C intervals between -30 and 30˚C

- Calculate **charge collected** at each bias point per temperature
- Fit charge against bias to calibrate temperature dependence on breakdown and operating bias ranges of these devices

Gradient gives change in bias per degree

- Estimate **+1.6 V/°C** change in FBK NLGADs
- Tested only with W4 (**shallow gain implant**)
  - **Expected to change** depending on implant design

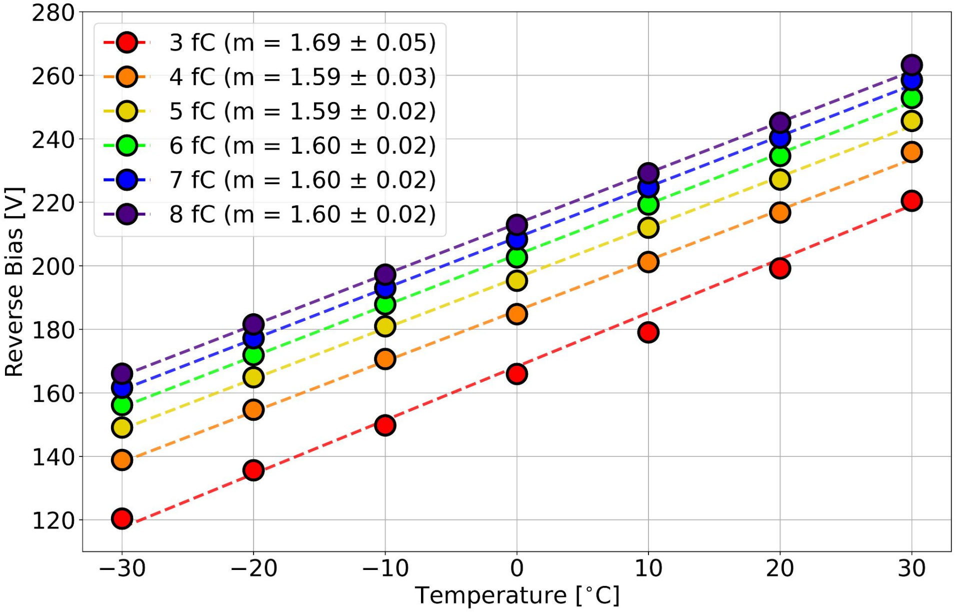

Ref. pLGAD result of -1 V/˚C for shallow *p*⁺ gain implant, -2 V/˚C for deep: [15] *Ferrero et. al., Intro to UFSDs*

- The n-type LGAD
- The FBK NLGAD batch of sensors
- Temperature characterisation of the FBK NLGAD batch
- **Operations at the DESY and CERN SPS Test Beam Facilities**
- Timing performances of the FBK NLGAD batch

Test beam setup

More details on each TB setup in backup

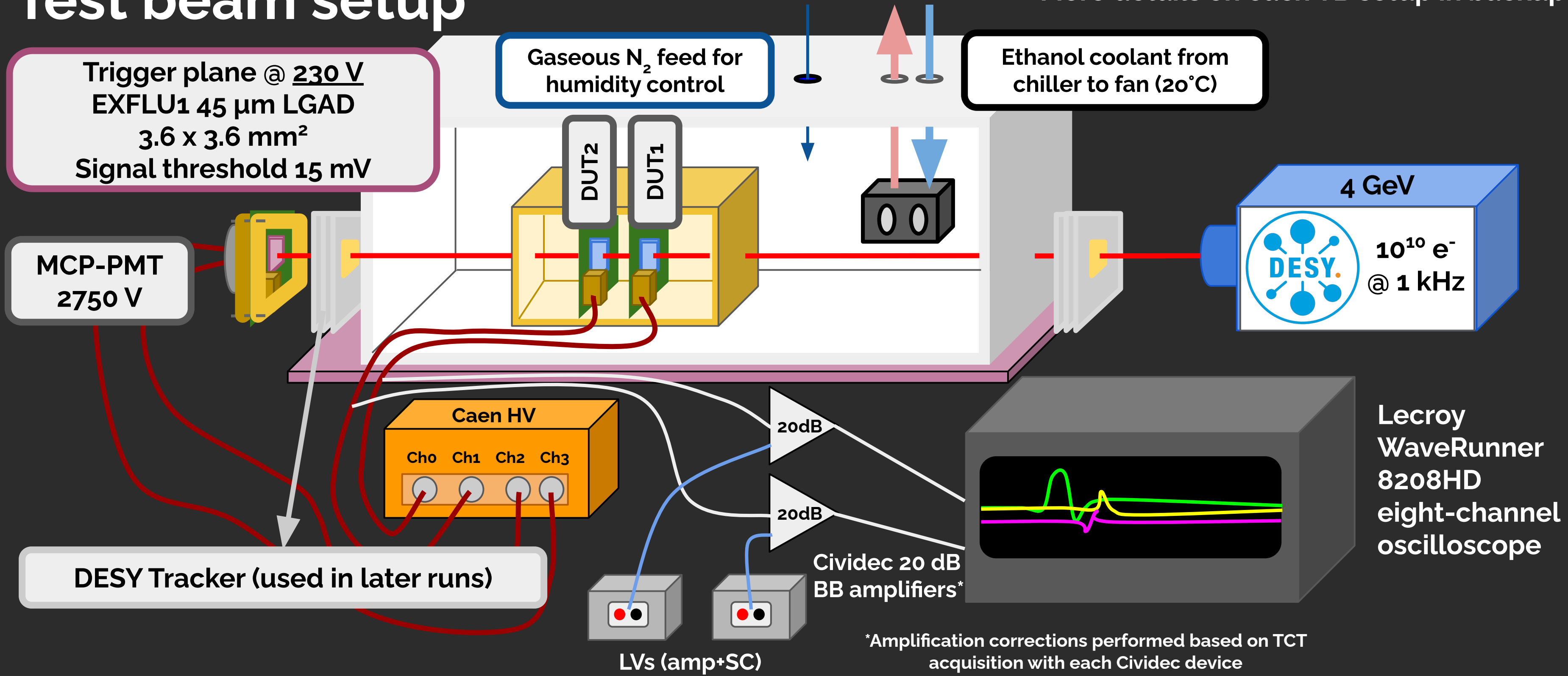

*Amplification corrections performed based on TCT acquisition with each Cividec device

TB name	Location	Date + Temp.	Raw acquisition BW
TB1	DESY TBF (4 GeV/c e^-)	Dec '25, ~20°C	4 GHz
TB2	CERN SPS (160 GeV/c π)	May '26, 22-25°C (*T-corr'd*)	2 GHz
TB3	**DESY TBF (4 GeV/c e^-)**	**July '26, fixed 20°C**	**1 GHz**

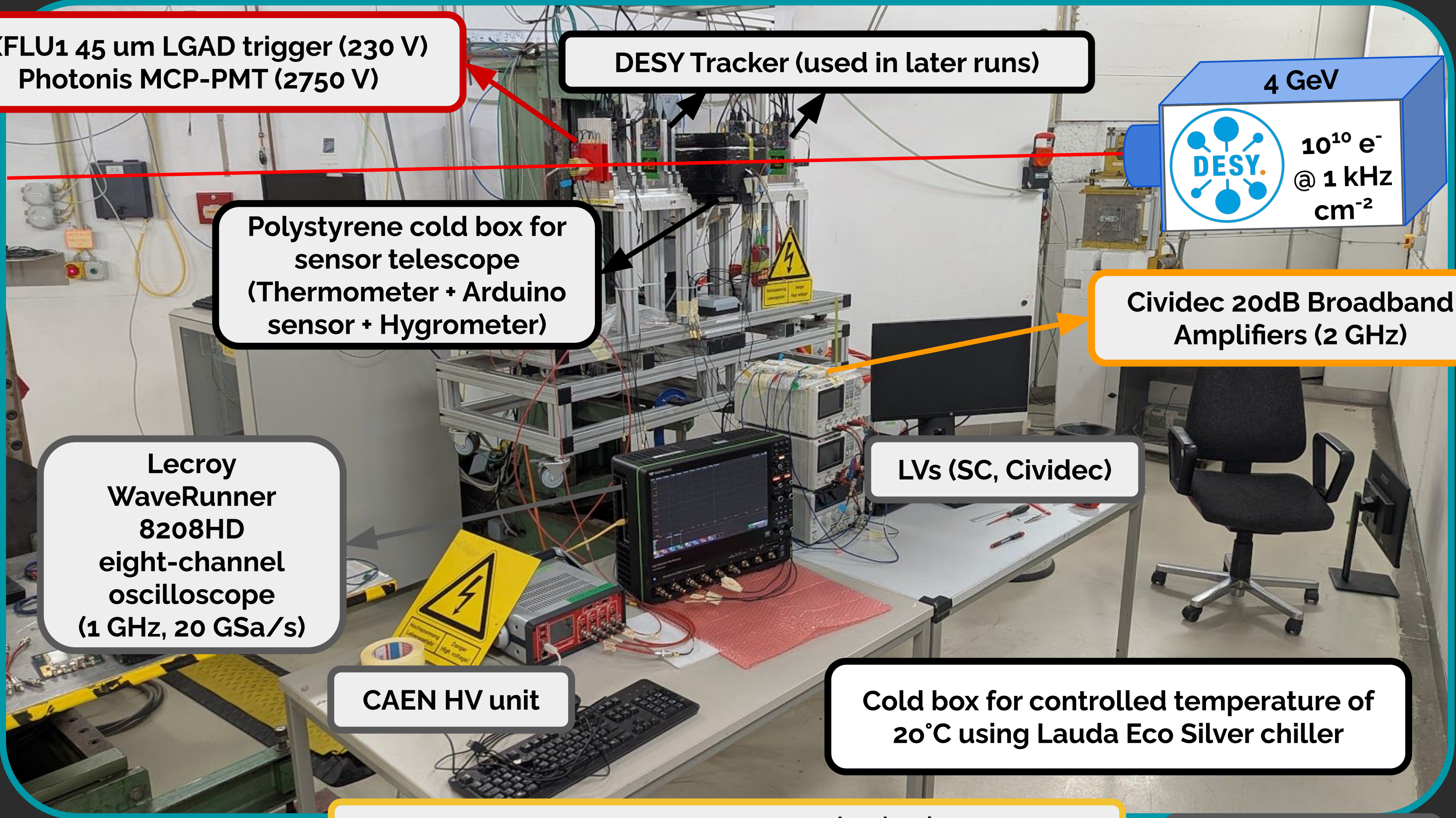

System BW_{NLGAD} ~0.9 GHz / $t_r^{inv\ signal}$ ~ 380 ps

TB3 setup shown

- The n-type LGAD
- The FBK NLGAD batch of sensors
- Temperature characterisation of the FBK NLGAD batch
- Operations at the DESY and CERN SPS Test Beam Facilities
- **Timing performances of the FBK NLGAD batch**

Typical distribution of area and amplitude

- At least 10k events per DAQ period
- Event filter to select signal
  - Cuts on area and amplitude to remove noise
  - MCP selection if signals saturate
- DUT-to-MCP coincidence between 10 and 13%
  - Trigger-to-MCP coincidence >99%
- For low biases and in breakdown, signal and noise are not always well separated
  - Further selections e.g. signal width required

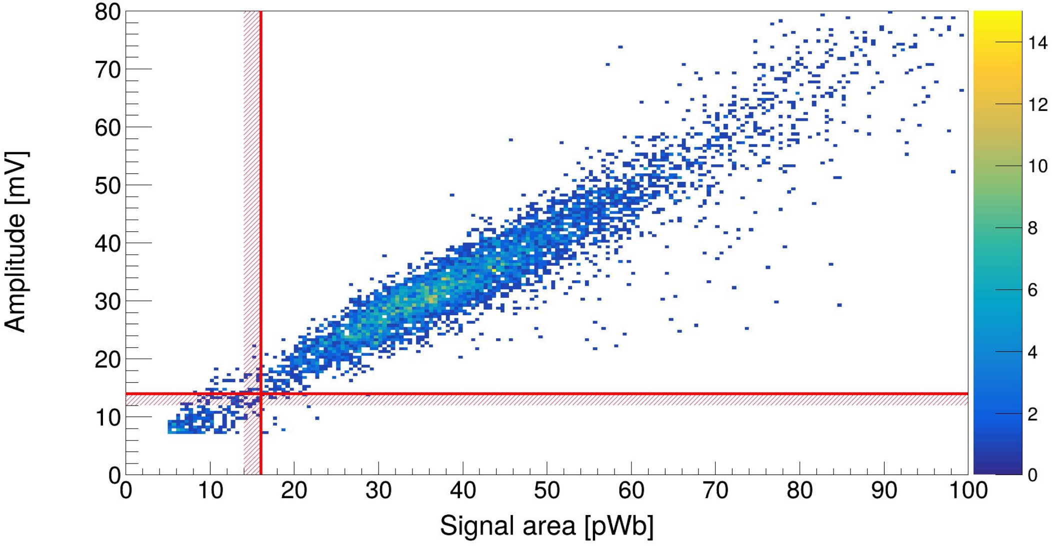

TB3 W4 @ 20°C under external reverse bias 245 V
(bulk of noise suppressed for better signal visualisation)

Collected charge *Q* extracted from Langaus fit to area

$$Q[\text{fC}] = \frac{10^3 \times \mathcal{A}[\text{pWb}]}{G_A R_{\text{in}}}$$

- R_{in} is 470 Ω in Santa Cruz boards*
- G_A ~10 (**correction for Cividec BB#3**)

Gain estimated from *Q* using formula**

$$Gain = 100[\mu\text{mfC}^{-1}]\frac{Q[\text{fC}]}{d_{\text{eff}}[\mu\text{m}]}$$

- d_{eff} effective substrate thickness ~55 µm

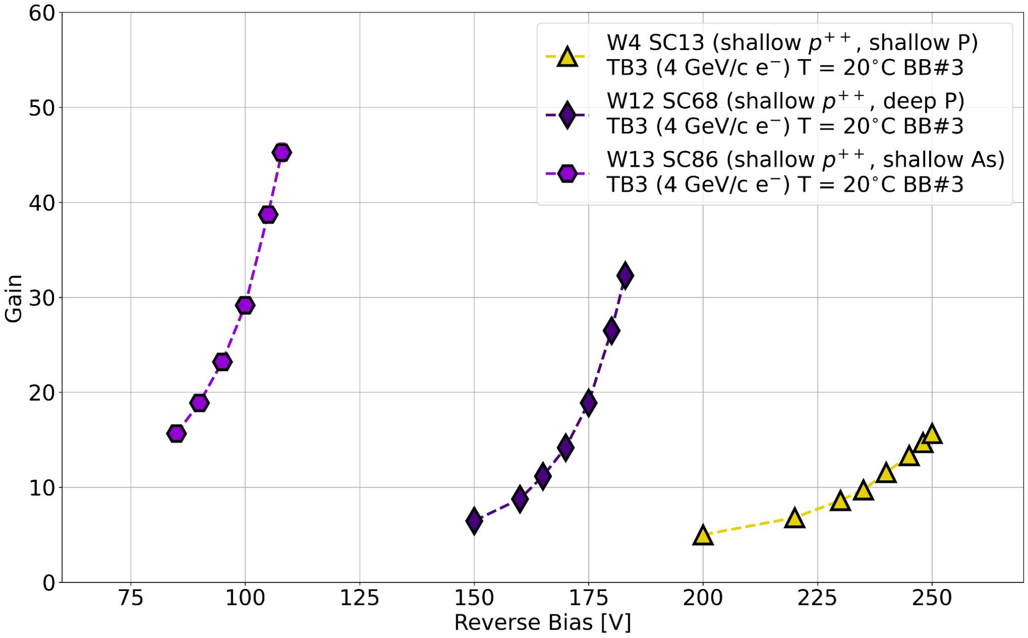

Gain in **NLGADs** consistent across TB campaigns, for e^- and p^+ beams

Refs.: [15] *Ferrero et. al., Intro to UFSDs*
[16] *R.S.White et. al., FBK EXFLU1 LGAD timing paper*

*50 Ω intrinsic with ~9.4 pre-amp gain in the SC board
**approximated from a MIP depositing 1 fC charge in 100 µm silicon

Results of TB3 at 20˚C (amplification corrections only, no bandwidth filter)

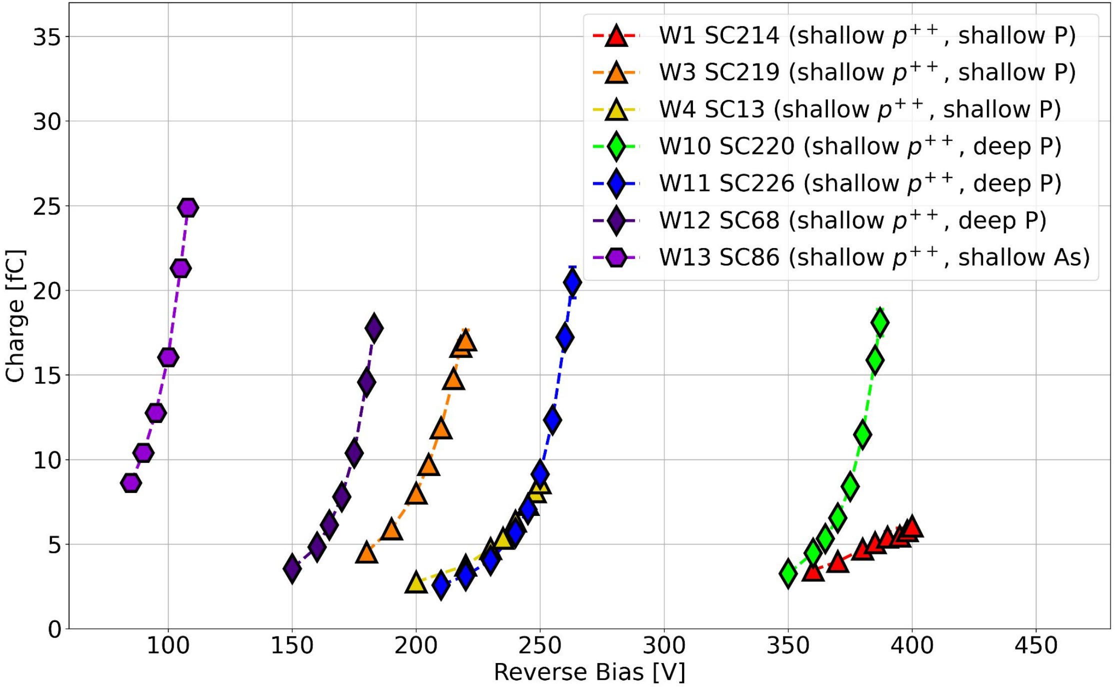

Charge varies between **3 and 25 fC**, corresponding to gain range of **5 to 46**
Operating bias range determined by wafer

Accounting for contributions to σ_t(DUT)

$$\sigma_t^2(\mathrm{DUT}) = \sigma_{\mathrm{jitter}}^2 + \sigma_{\mathrm{ionisation}}^2 + \sigma_{\mathrm{distortion}}^2 + \sigma_{\mathrm{digitisation}}^2$$

≈0

- Dominant terms are **jitter** and **ionisation**
  - **Digitisation** negligible using CFD w/ 20 GSa/s
  - **Distortion** of signal from non-saturated v_{drift}, ***assumed negligible >200 V*** for these NLGADs

$$\sigma_{\mathrm{jitter}} = \frac{N}{\frac{\mathrm{dV}}{\mathrm{dt}}} \simeq \frac{t_{\mathrm{rise}}}{\frac{S}{N}}$$

σ_{jitter} decreases with charge, reaching sub-20 ps

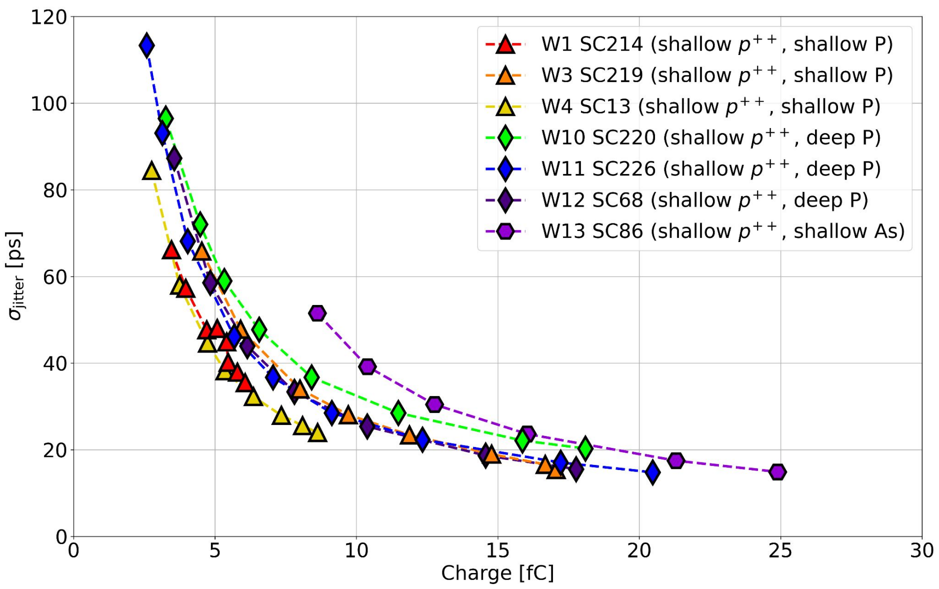

Refs.: [15] *Ferrero et. al., Intro to UFSDs*
[16] *R.S.White et. al., FBK EXFLU1 LGAD timing paper*

Timing resolution σ_t(DUT) computation

- Gaussian fit to difference in arrival time at **30%** threshold on rising edge (**CFD**)
- Extracted using the formula

$$\sigma_t(\mathrm{DUT}) = \sqrt{\sigma_t^2(\mathrm{DUT};\mathrm{MCP}) - \sigma_t^2(\mathrm{MCP})}$$

Beam Test	σ_t(MCP)
DESY (TB1, TB3)	7.0 ± 2.8 ps
SPS (TB2)	9.6 ± 1.8 ps

- Estimated in a **tri-plane setup with 20 µm EXFLU1 sensors**
- Average value over series of bias points

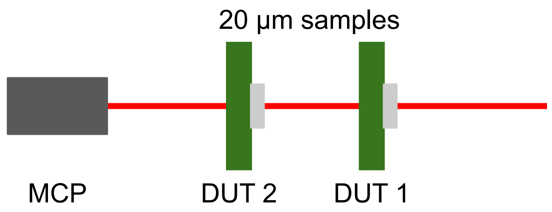

$$\sigma_t(\mathrm{MCP}) = \frac{1}{\sqrt{2}}\sqrt{\sigma_t^2(\mathrm{DUT1};\mathrm{MCP}) + \sigma_t^2(\mathrm{DUT2};\mathrm{MCP}) - \sigma_t^2(\mathrm{DUT1};\mathrm{DUT2})}$$

$$\sigma_t^2(\mathrm{DUT1};\mathrm{MCP}) = \sigma_t^2(\mathrm{DUT1}) + \sigma_t^2(\mathrm{MCP})$$

$$\sigma_t^2(\mathrm{DUT2};\mathrm{MCP}) = \sigma_t^2(\mathrm{DUT2}) + \sigma_t^2(\mathrm{MCP})$$

$$\sigma_t^2(\mathrm{DUT1};\mathrm{DUT2}) = \sigma_t^2(\mathrm{DUT1}) + \sigma_t^2(\mathrm{DUT2})$$

Ref.: [16] *R.S.White et. al., FBK EXFLU1 LGAD timing paper*

Timing resolution σ_t(DUT) for **FBK NLGADs**

- Data from TB3 only
- Roughly group with the **wafer type**, with the exception of W3
- σ_t(DUT) reaches **62.6 ± 0.7 ps** at best, for as little as **8 fC** in W4 and **17 fC** in W3 and W11

σ_t(DUT) intrinsically **higher** in NLGADs

- Higher shot noise
- Higher E-field for multiplication
- **Sub-40 ps in 55 µm FBK *p*-type LGADs**

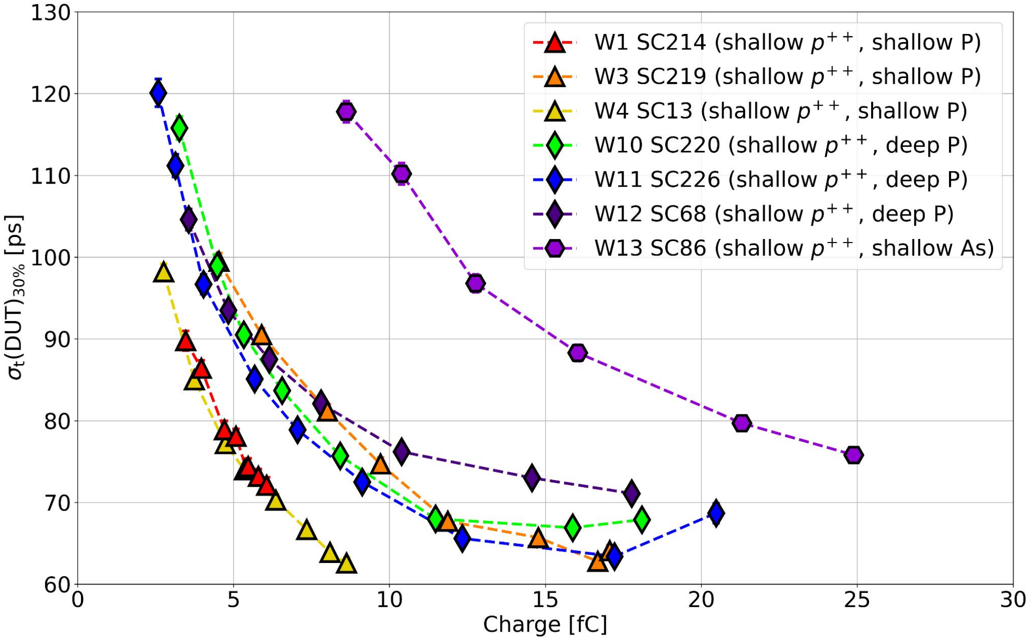

Refs.: [6] [M. Moll, TCAD simulation of impact ionisation]
[7] [E. Rivera, M. Moll, Impact ionisation coefficients in LGADs]
[8] [C. Canali et. al., Hole drift velocity in silicon]
[17] [F. Siviero et. al., Timing performance of 55 µm pLGADs]

Contribution from **non-uniform ionisation** invariant of charge

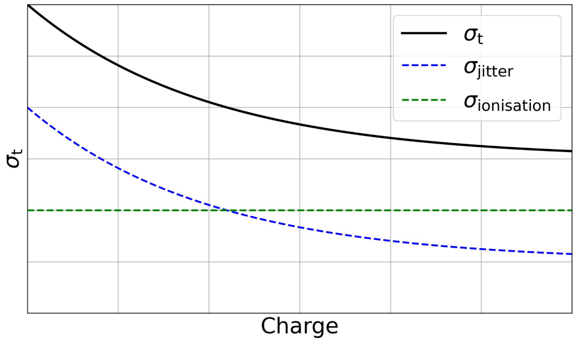

- Calculated from minimum σ_t(DUT)
- **Dominant** contribution to σ_t(DUT) above 10 fC

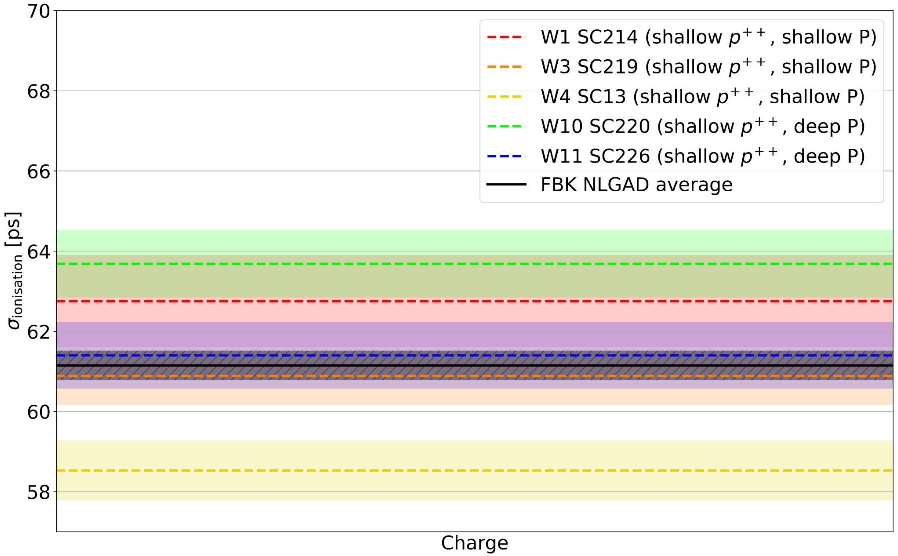

Wafers with lower operating bias ranges (W12, W13) omitted

Refs.: [15] *Ferrero et. al., Intro to UFSDs*
[16] *R.S.White et. al., FBK EXFLU1 LGAD timing paper*

Outlook for the FBK NLGAD batch

- Additional measurements for **temperature characterisation** of non-irradiated NLGADs
- Studies ongoing with the **irradiated NLGADs**
- **X-ray analysis** ongoing for soft photon detection
- **TPA-TCT studies** ongoing to characterise the gain region and charge carrier behaviour
- **Charge screening** studies ongoing with TCT laser and ^{241}Am sources

Converging on product specifications for the **FBK CompleX1 batch** of compensated LGADs

Thank you for your attention

[1] HL-LHC - radiation conditions following LHC upgrade

[2] CMS - tracker environment for HL-LHC

[3] ATLAS - tracker upgrade for HL-LHC

[4] FCC-hh - FCC *hh* collisions and resulting ambient radiation

[5] G. Pellegrini et. al., LGADs for HEP applications

[6] M. Moll, TCAD simulation of impact ionisation

[7] E. Rivera, M. Moll, Impact ionisation coefficients in LGADs

[8] C. Canali et. al., Hole drift velocity in silicon

[9] M. Centis Vignali, G. Paternoster, LGADs for photon science

[10] J. Villegas et. al., CNM nLGADs with low-penetrating particles

[11] The path to the extreme fluences via the nLGAD sensors

[12] Results from the first 55 µm thick nLGAD sensors from FBK

[13] Characterisation of the first 55 µm thick nLGAD sensors from FBK

[14] A. R. et. al., Periphery layout strategies to mitigate discharges

[15] M. Ferrero et. al., An Introduction to Ultra-Fast Silicon Detectors

[16] R.S.White et. al., FBK EXFLU1 LGAD timing paper

[17] F. Siviero et. al., Timing performance of 55 µm pLGADs

We acknowledge the following funding agencies and collaborations:

- ▻ INFN CSN5
- ▻ RD50 and DRD3, CERN
- ▻ Ministero della Ricerca, Italia, PRIN 2022, progetto 2022RK39RF – ComonSens

This work is supported by the European Union (ERC), CompleX, Grant Agreement No 101124288, and Next Generation EU, Mission 4 Component 1 CUP D53D23002870001, ComonSens.

Views and opinions expressed are, however, those of the authors only and do not necessarily reflect those of the European Union or the European Research Council. Neither the European Union nor the granting authority can be held responsible for them.

The measurements leading to these results have been performed at the Test Beam Facility at DESY, Hamburg (Germany), a member of the Helmholtz Association (HGF).

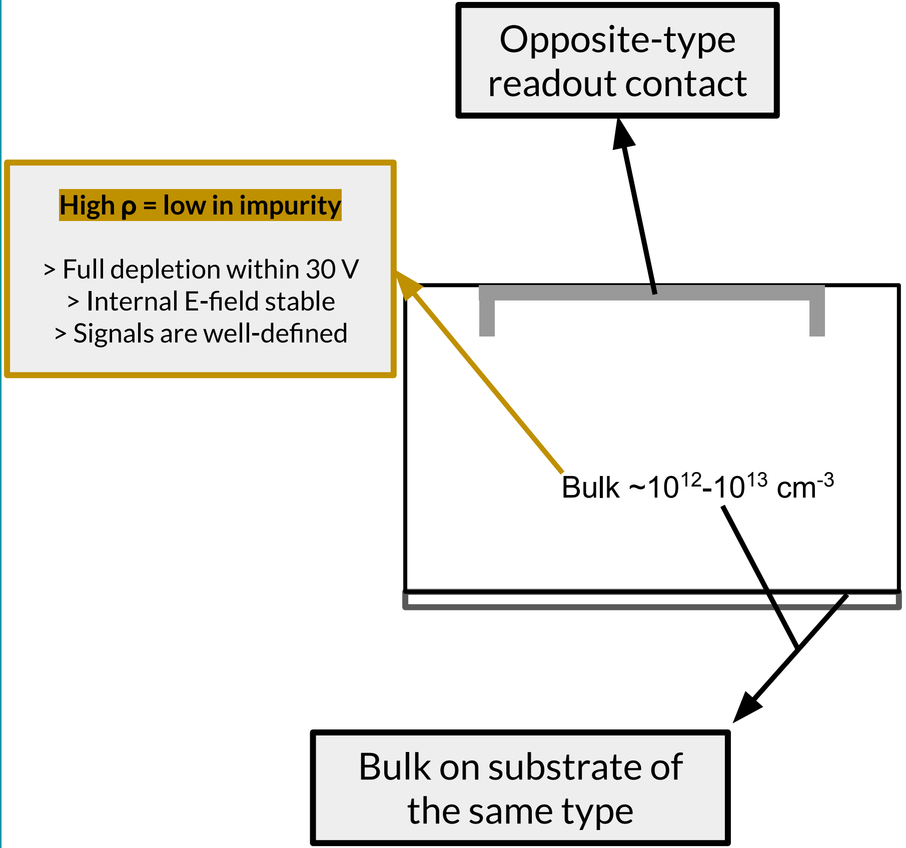

An **LGAD** is similar to a PiN diode

- Si bulk with high resistivity ρ

Bulk thickness of *O*(10 μm)

Ref.: [5] *Pellegrini et. al., LGADs for HEP applications*

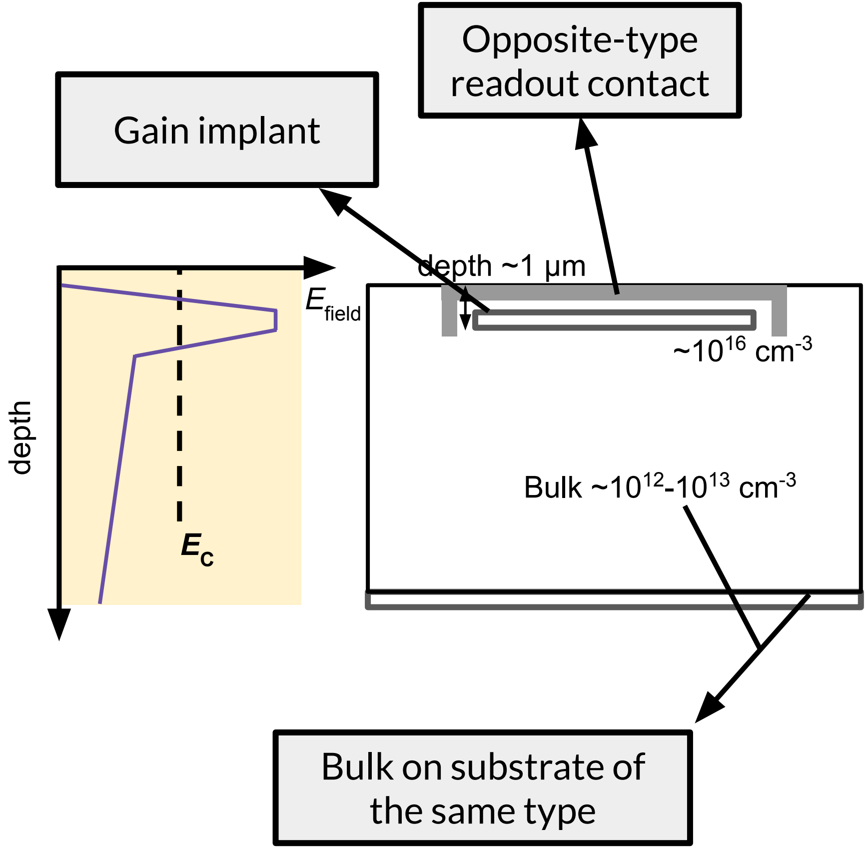

An **LGAD** is similar to a PiN diode

- Si bulk with high resistivity ρ
- Implant a highly concentrated layer ~10^{16} cm^{-3}
  - E-field will peak around this region under an external reverse bias

Bulk thickness still *O*(10 μm)

Ref.: [5] *Pellegrini et. al., LGADs for HEP applications*

Reference for wafers

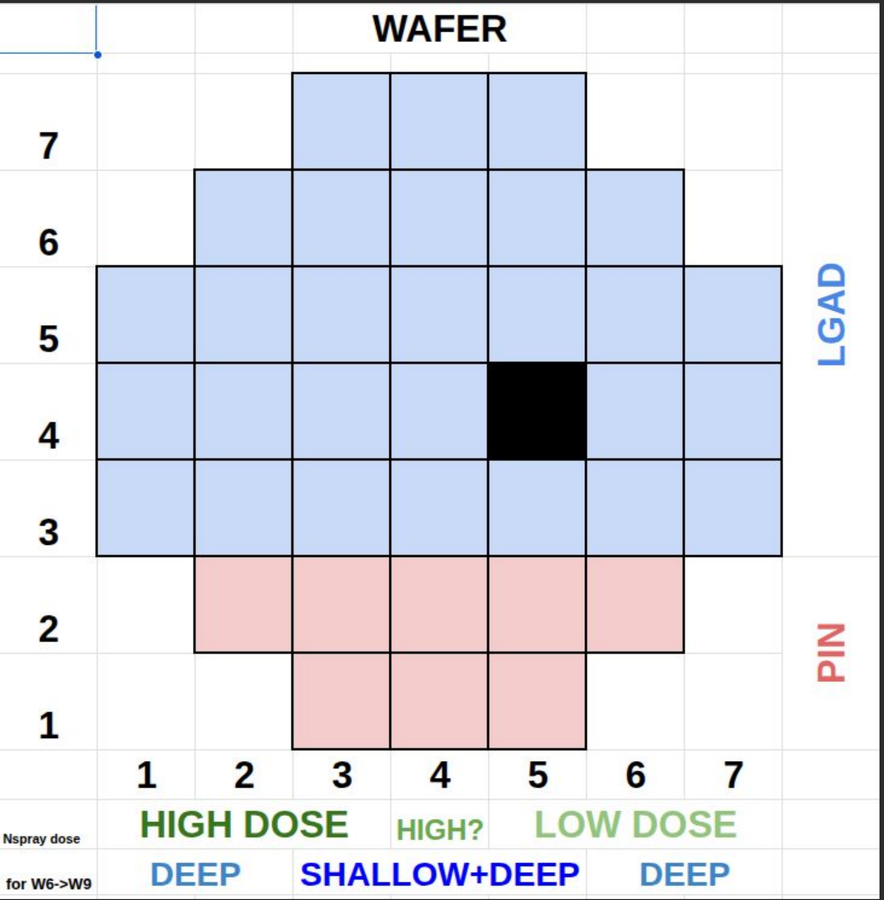

SP1 S1	SP2 S2	SP3 S3 NM	SP4 S4	SP5 S5
SP6 S6	SP7 S7	SP8 S8	SP9 S9	SP10 S10
BP11 S3 NM	BP12 S1	BP13 S2	BP14 S4	BP15 S10
LP16 S1	LP17 S2	LP18 S7	LP19 S8	LP20 S10
2x2-21 S1	2x2-22 S2	2x2-23 S7	2x2-24 S10	T25 TEST

Guard Ring Type					
Name	Type	Design			
S1	GR0 5um	5 um NCUTW 200 um GR0 FULL NSTOP			
S2	GR0 10um	10 um NCUTW 200 um GR0 FULL NSTOP			
S3	GR0 5um NM	5 um NCUTW 200 um GR0 FULL NSTOP			
S4	GR1 5um 74	5 um NCUTW 150 um GR1 74 FULL NSTOP			
S5	GR1 5um 74 NONS	5 um NCUTW 150 um GR1 74			
S6	GR1 5um 74 RING	5 um NCUTW 150 um GR1 74 NSTOP RINGS			
S7	GR1 10um 74	10 um NCUTW 150 um GR1 74 FULL NSTOP			
S8	GR1 5um 34	5 um NCUTW 150 um GR1 34 FULL NSTOP			
S9	GR1 5um 24	5 um NCUTW 150 um GR1 24 FULL NSTOP			
S10	GR3 10um	10 um NCUTW 90 um GR3 FULL NSTOP THIN CCR			

Wafer	Contact	Gain	n^+ dose
1	Shallow	Phosphorus shallow	1.20
2			1.26
3			1.30
4			1.36
5			1.40
6	Deep or Shallow+Deep	Phosphorus deep	1.30
7			1.36
9			1.40
10	Shallow		0.90
11			0.96
12			1.00
13		Arsenic shallow	1.30
14			1.36
15			1.40

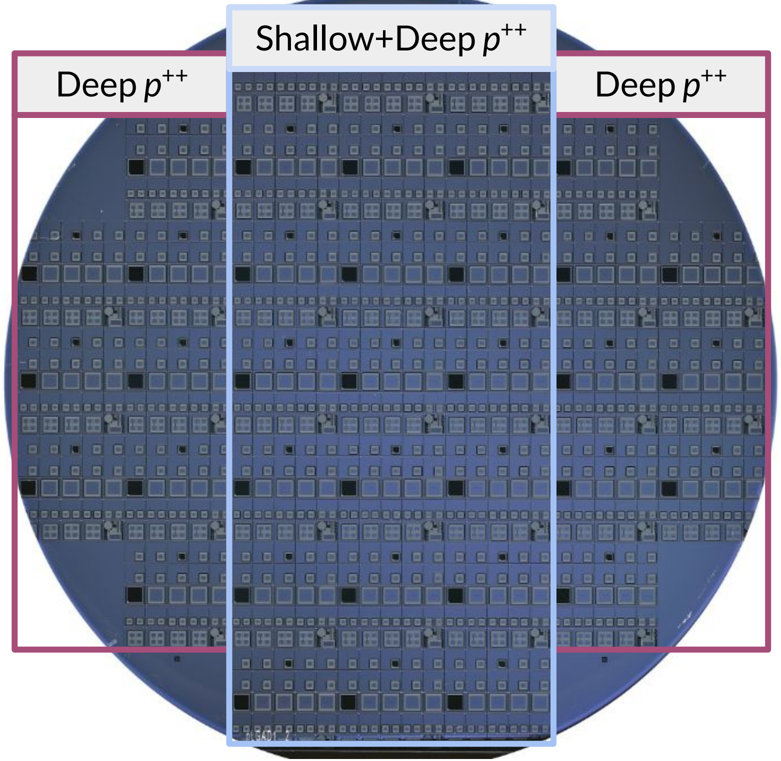

FBK NLGAD wafer

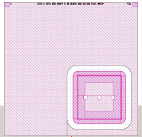

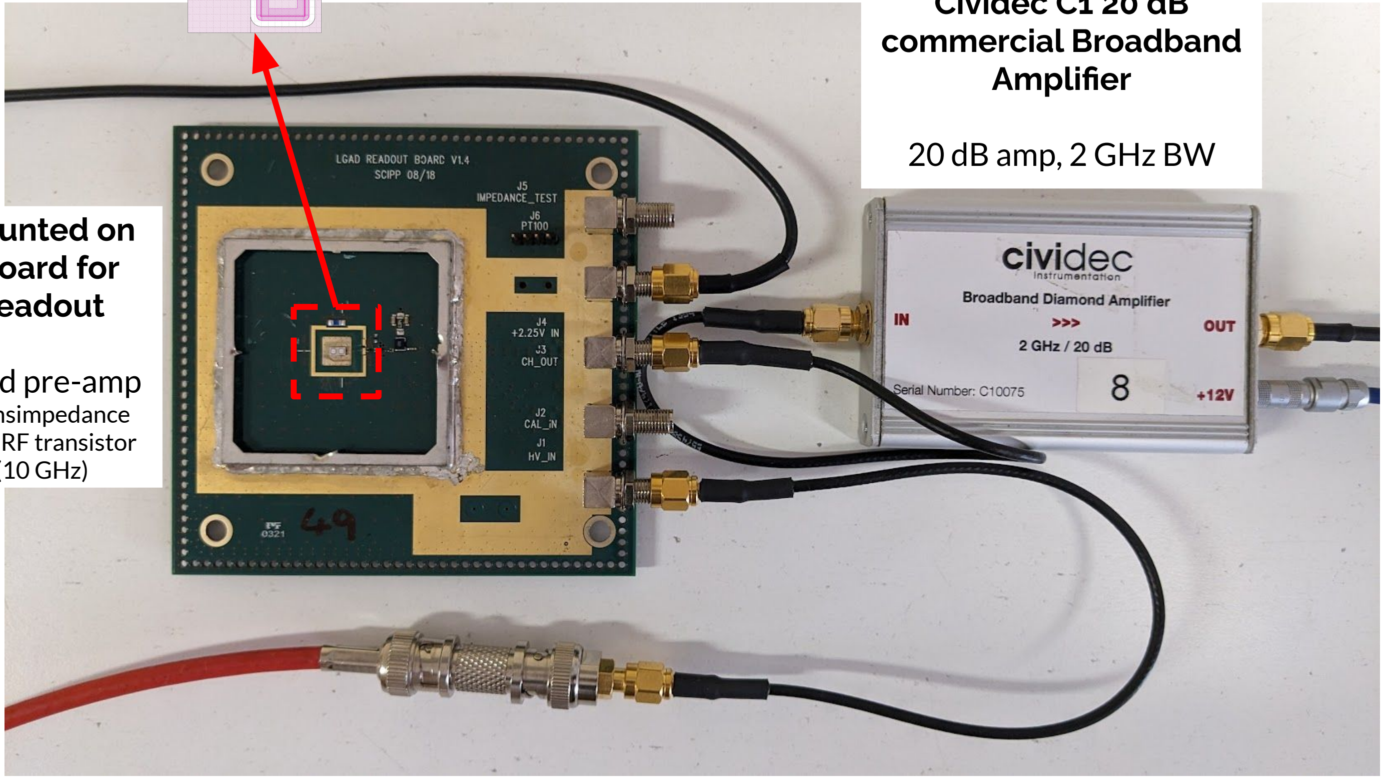

SC -> LV
+2.25 V

LGAD-PIN mounted on Santa Cruz board for electronic readout

20 dB integrated pre-amp
470 Ω inverting transimpedance amp + Infineon SiGe RF transistor supports BW O(10 GHz)

SC -> HV
Up to 400 V
external reverse bias

Cividec C1 20 dB commercial Broadband Amplifier

20 dB amp, 2 GHz BW

Amp -> Osc
Inverted signal

LV -> Amp
+12 V

DESY TBF *TB1* beamline setup

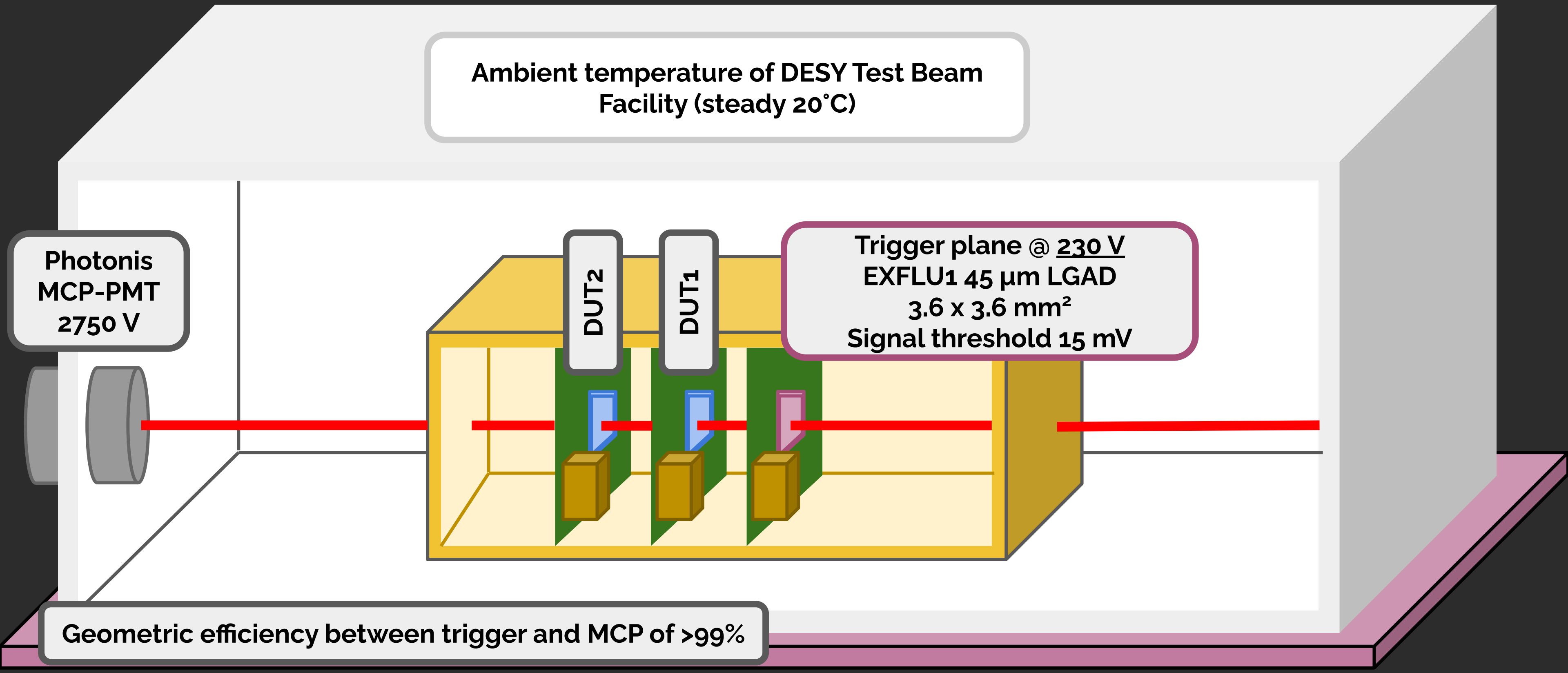

CERN SPS *TB2* beamline setup

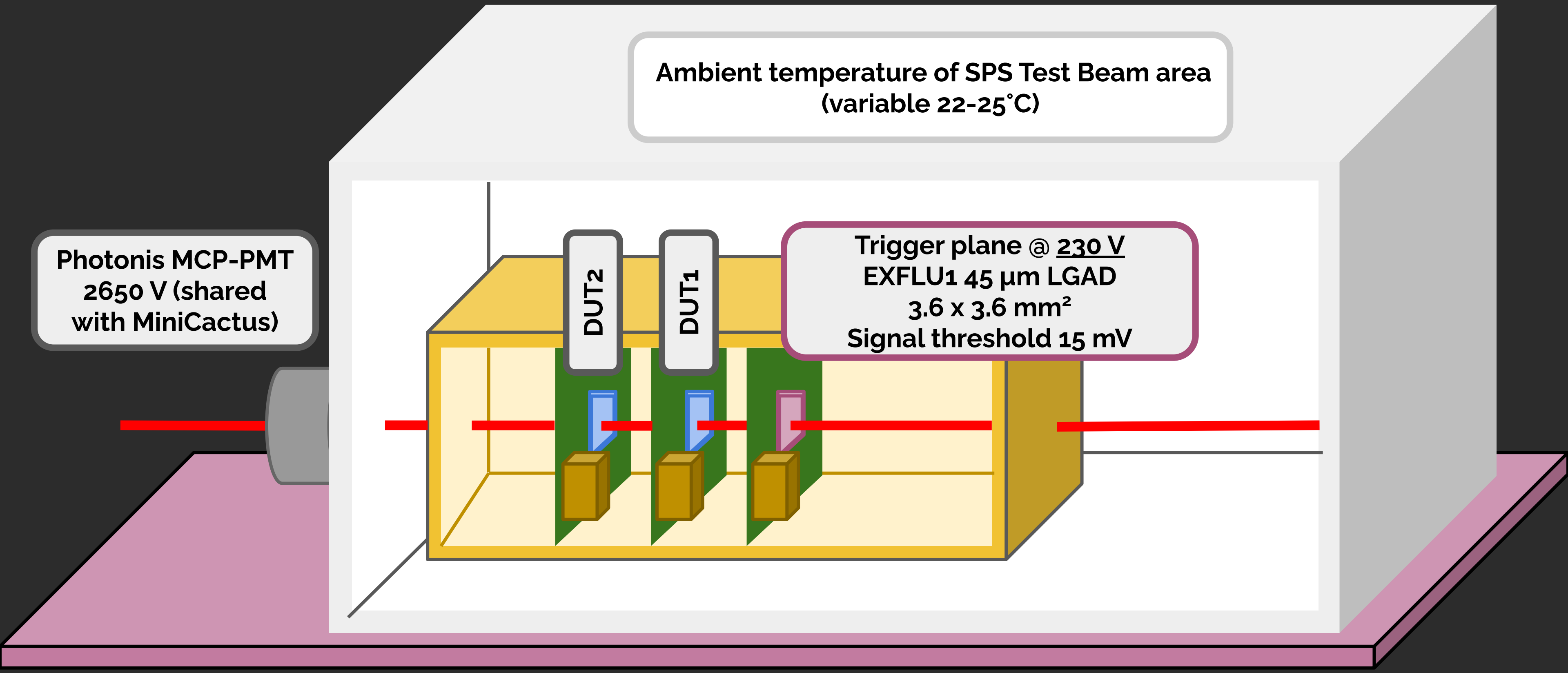

DESY TBF *TB3* beamline setup

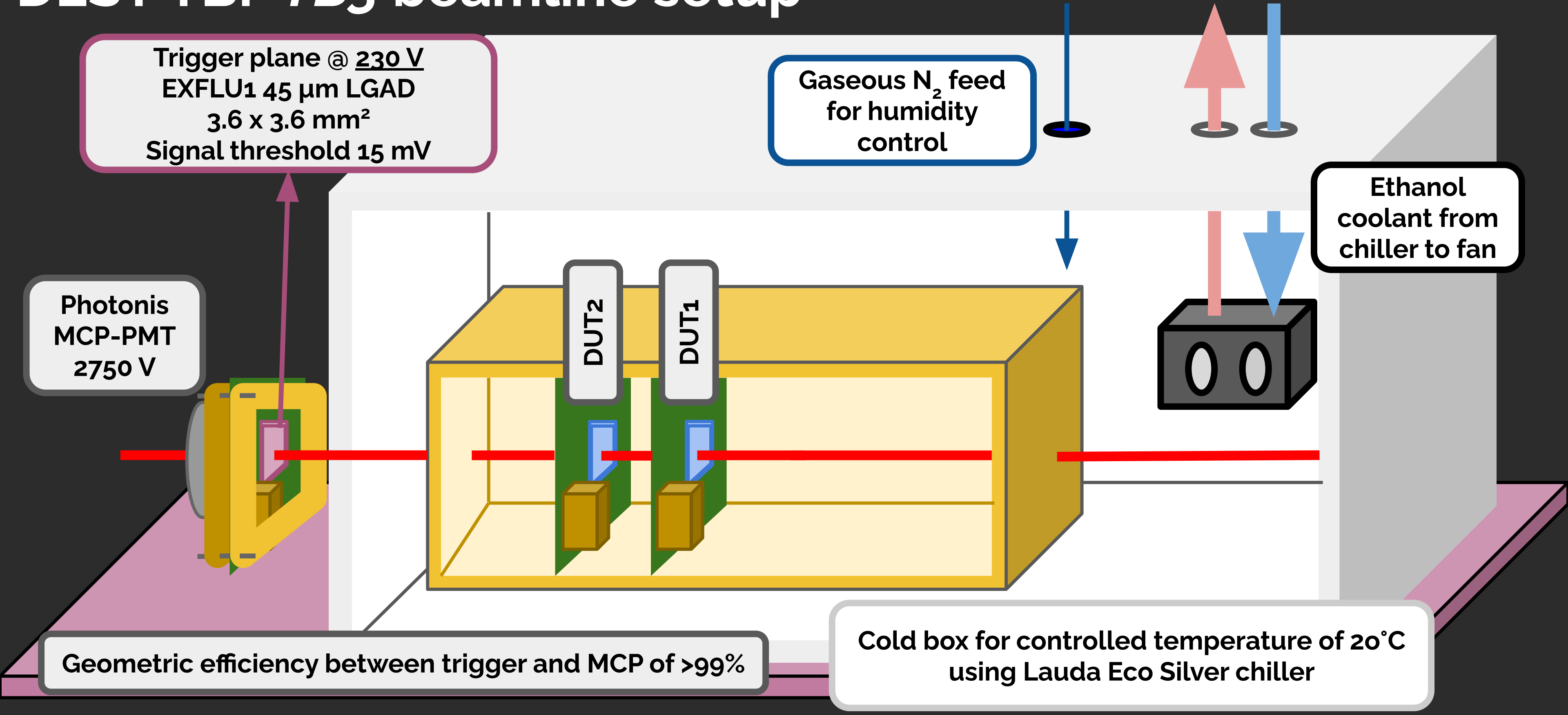

Results of TB3 at 20˚C (amplification corrections only, no bandwidth filter)

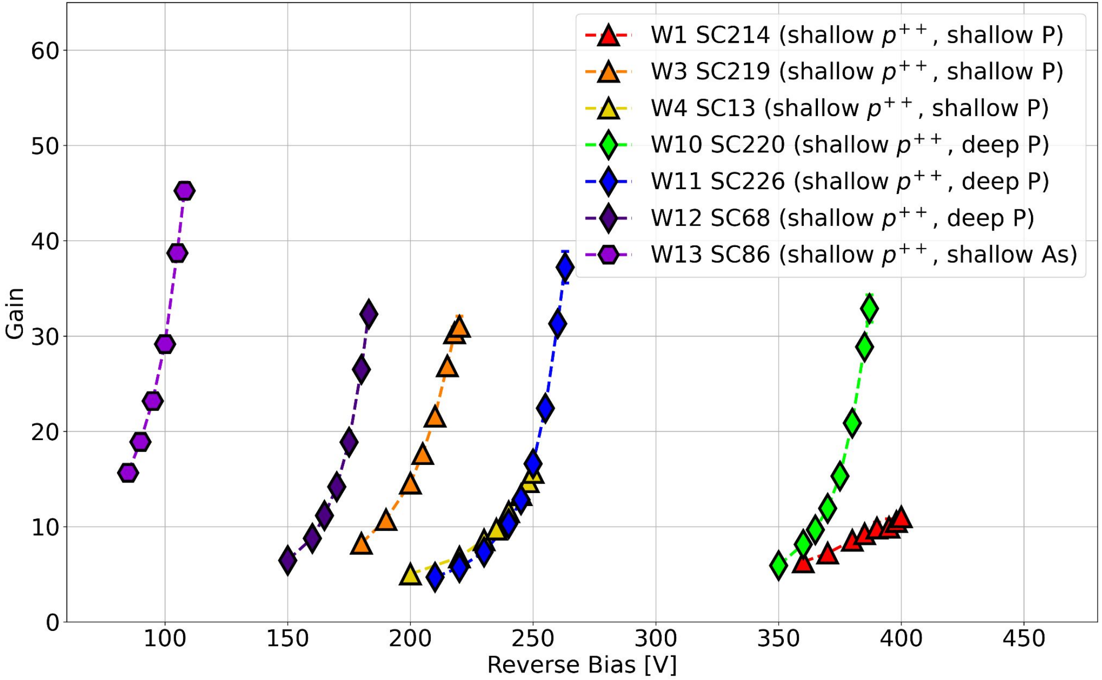

Charge varies between **3 and 25 fC**, corresponding to gain range of **5 to 46**
Operating bias range determined by wafer

Results of TB3 at 20˚C (amplification corrections only, no bandwidth filter) - RMS noise

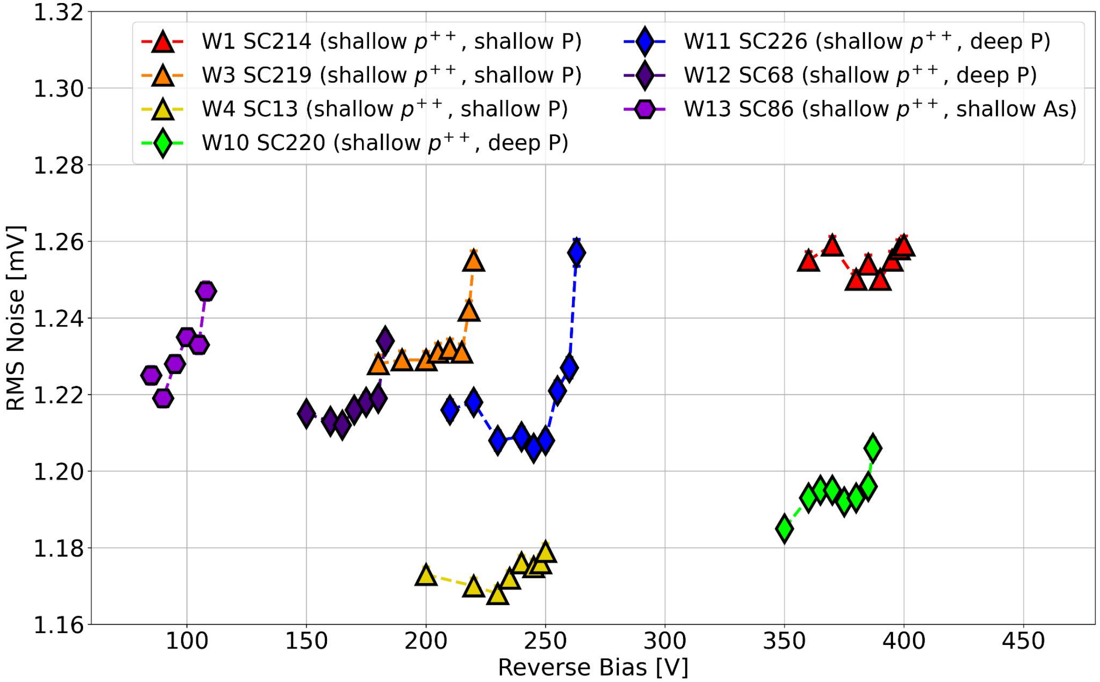

RMS baseline noise increases sharply just at breakdown

Saturation of charge carriers corresponds to the rise time stabilising

- In **LGADs** such as the EXFLU1 batch, these tend to be stable across a large V_{bias} range near breakdown
- Rising edge from e^- drifting through bulk, for which v_{drift} saturates under a bulk E-field strength of **3 Vμm^{-1}**
- In **NLGADs**, rising edge determined by h^+, for which v_{drift} **saturates closer to 5-10 Vμm^{-1}**

For higher V_{bias} (so higher bulk E-field strength), the **rise time appears to plateau** in NLGADs

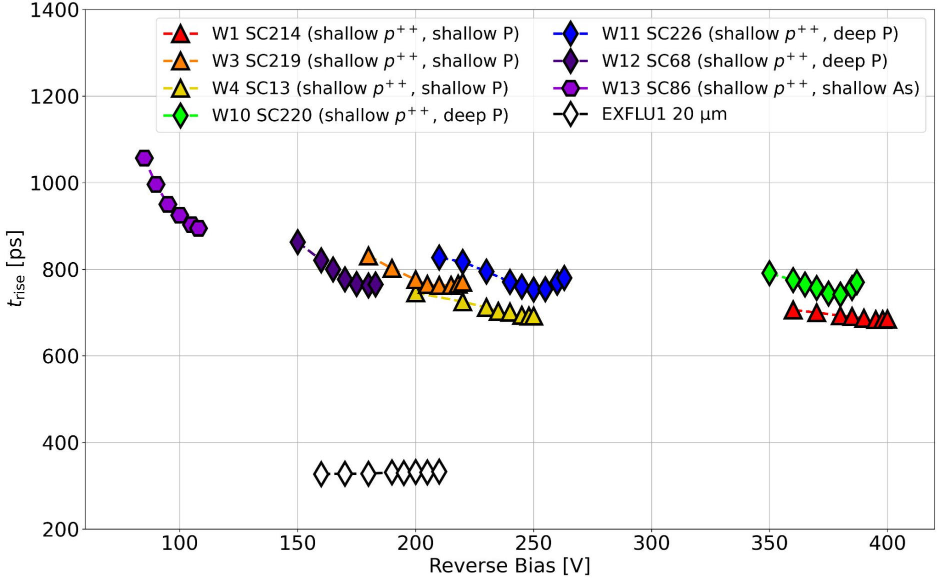

Refs.: [8] *C. Canali et. al., Hole drift velocity in silicon*

Saturation of charge carriers can be probed from the relation between amplitude and area of the waveforms

- If they are linearly related, v_{drift} is closer to being saturated
- Deviation from linearity indicates that the waveforms are not well-correlated between the area under the curve and the amplitude
- Saturation achieved easily with 20 um EXFLU1 LGADs (e^- drift saturates)
- Hole drift velocity does not saturate below 300 V in 55 um NLGADs, but is expected to be sufficiently stable above 200 V

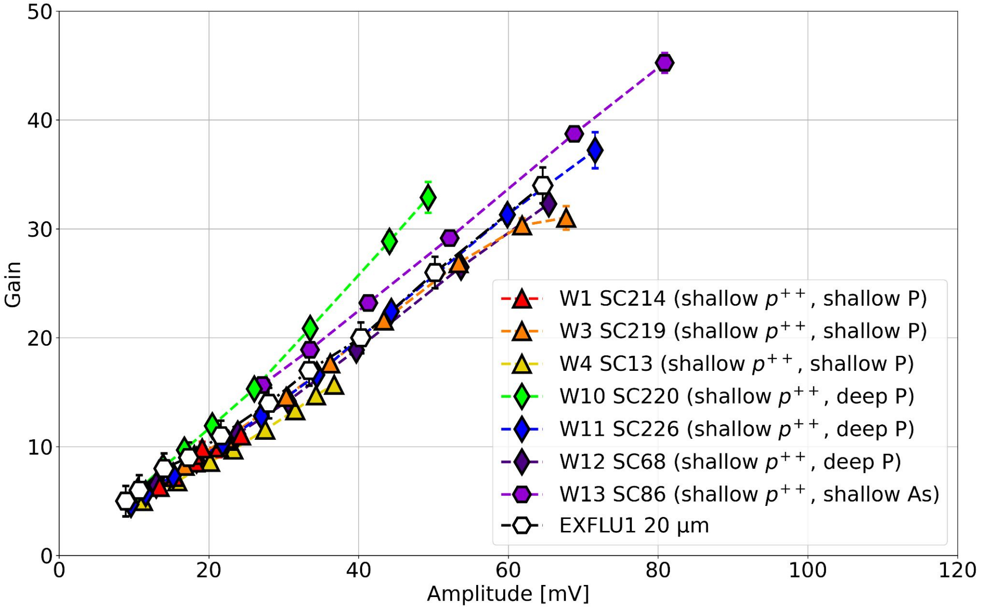

Refs.: [8] *C. Canali et. al., Hole drift velocity in silicon*